Cretaceous Research 102 (2019) 59–80

Contents lists available at ScienceDirect

Cretaceous Research

journal homepage: www.elsevier.com/locate/CretRes

Aptian–early Albian sedimentation in the Essaouira-Agadir basin, Western Morocco

Etienne Jaillard [a, *], Walid Hassanein Kassab [b], Fabienne Giraud [a], Emmanuel Robert [c], Moussa Masrour [d], Lhoussaine Bouchaou [d], Khadija El Hariri [e], Mohamed S. Hammed [b], Mohamed F. Aly [b]

[a] Université Grenoble Alpes, ISTerre, IRD, CNRS, IFSTTAR, CS 40700, 38058 Grenoble Cedex 9, France
[b] Earth Science Department, Cairo University, Gizah, Egypt
[c] Université Lyon 1, ENS Lyon, CNRS, UMR 5276 LGLTPE, 69622 Villeurbanne, France
[d] Université Ibn Zohr, Faculté des Sciences, Département de Géologie, Laboratoire LAGAGE, BP 8106, Cité Dakhla, Agadir, Morocco
[e] Université Cadi Ayyad, Faculté des Sciences et Techniques-Guéliz, Département Sciences de la Terre, Avenue Abdelkrim el Khattabi, BP 549, 40000 Marrakech, Morocco

ARTICLE INFO

Article history:
Received 5 November 2018
Received in revised form
1 April 2019
Accepted in revised form 17 April 2019
Available online 25 April 2019

Keywords:
Early Cretaceous
Sedimentology
Sequence stratigraphy
Paleoenvironment
Paleogeography

ABSTRACT

Aptian to early Albian times were marked by various geodynamic and paleoenvironmental events such as large igneous province volcanism, perturbations of climate and the carbon cycle, and sea-level changes. The Essaouira-Agadir basin (EAB), located on the Atlantic passive margin of Morocco, offers good and fossiliferous exposures of the Aptian–Albian sedimentary series. A detailed analysis of this succession made it possible to establish a biostratigraphic framework. The identification of discontinuities allowed to define eight depositional sequences. As most of them are correlatable with depositional sequences of other Tethyan areas, they suggest that eustacy was the main parameter controlling sedimentation. The analysis of sedimentary facies and nannofossil assemblages provides information on paleoenvironmental changes.

Sedimentation in the EAB evolved from a very low energy, carbonate ramp in the early Aptian to a low energy, slightly deeper, mixed carbonate-clastic ramp in the early Albian. This change occurred along with an increase of clastic input, a change from oligotrophic to mesotrophic faunal assemblages, and a decrease of sea-surface temperatures. The occurrence of current sedimentary features, sporadic dysaerobic deposits and local phosphatic and glauconitic crusts suggests that upwelling currents were significant during this period.

Paleogeographic and isopach maps support a transgressive trend in the late Aptian and early Albian, and unravel subsidence anomalies suggesting mild halokinetic movements during Aptian–early Albian times.

1. Introduction

The Aptian to early Albian was an interval of important oceanographic, climatic and geodynamic changes. In fact, this period recorded the earliest significant Oceanic Anoxic Event (OAE) of the Cretaceous crises in the biological and/or carbon cycles, resulting in deposition of organic-rich "black shales" (e.g. Schlanger and Jenkyns, 1976; Giorgioni et al., 2015). The rifting and opening of the Atlantic ocean at equatorial latitudes (e.g. Moulin et al., 2010; Klingelhoefer et al., 2016) opened new N–S oceanic connections, whereas the former Tethyan system was dominated by E-W oceanic circulations. A warm climate, related to the greenhouse effect (Föllmi, 2012) was followed by significant cooling of the global ocean and climate in the late Aptian (Bottini et al., 2015). The emplacement of large igneous provinces influenced global climate (Kuroda et al., 2011). Noticeable, widespread lower Aptian carbonate shelves developed during the early Aptian (e.g. Skelton and Gili, 2012), and a significant sea-level fall in the early Aptian was followed by a marked late Aptian–early Albian sea-level rise recorded in most areas around the world (Haq, 2014). Therefore,

* Corresponding author.
E-mail address: Etienne.Jaillard@univ-Grenoble-Alpes.fr (E. Jaillard).

https://doi.org/10.1016/j.cretres.2019.04.008
0195-6671/

sedimentary record of the Aptian–lower Albian has been extensively studied in the North-Tethyan margin, but remains relatively poorly studied elsewhere. The Aptian–lower Albian succession is poorly known in northern Africa, likely because it consists either of carbonate shelf, or of sand-rich deposits poor in ammonites (e.g. Burollet, 1956; Vila, 1980), or of shelf marls rich in endemic ammonite fauna (e.g. Latil, 2011; Robert in; Peybernès et al., 2013; Luber et al., 2017). The Western Atlas of Morocco offers a good opportunity for studying the Aptian–lower Albian, seeing that good exposures of fossiliferous successions are easily accessible.

We did a stratigraphic and sedimentological study of the Aptian–lower Albian deposits of the Essaouira-Agadir Basin (EAB), which constitutes the Western end of the Atlas chain (Fig. 1). Here, we present a preliminary biostratigraphic scheme, a detailed sedimentological analysis mainly based on field observations along thirteen sections distributed in the central and southern parts of the EAB, a sequence stratigraphic interpretation of this succession and a paleogeographic synthesis of the sedimentary evolution of the basin. In order to better constrain paleoenvironments, we provide additional data on calcium carbonate content, total organic carbon (TOC) and calcareous nannofossils. These data are compared to sedimentary facies to better understand the temporal and spatial relationships between carbonate production, primary productivity, oxygenation of the water column, and organic carbon burial during changes in both sea-surface temperature and sea level.

2. Geological background

The EAB (Fig. 1) belongs to the Atlantic passive margin. Its Mesozoic sedimentary history began with the Tethyan rifting, which eventually provoked the opening of the Central Atlantic (Zühlke et al., 2004; Hafid et al., 2008; Schettino et al., 2009). Therefore, it has been marked by strong extensional tectonics from late Permian to early Liassic times, coeval with deposition of thick red beds, overlain by shales and evaporites interbedded with basaltic flows, and sealed by a pre-Pliensbachian unconformity (Hafid, 2000). An extensional regime prevailed until the Late Cretaceous, and favoured the deposition of shallow marine deposits in the EAB. Shelf carbonates deposition prevailed during the Jurassic and was interrupted by regressions in Middle and latest Jurassic times (Stets, 1992), due to the general uplift of the High Atlas (Frizon de Lamotte et al., 2008). The Early Cretaceous is marked by the deposition of thick, mainly marly marine deposits, sporadically interrupted by clastic deposits deriving from the East (late Hauterivian, late Barremian; Canérot et al., 1986; Rey et al., 1988; Witam, 1998; Masrour et al., 2004; Al Yacoubi et al., 2017). Aptian to Turonian times are represented by marine, marly and calcareous strata (Ambroggi, 1963; Bourgeoini et al., 2002; Ettachfini et al., 2005; Jati et al., 2010; Peybernès et al., 2013). The Upper Cretaceous mainly calcareous sedimentation (Andreu, 1989) was then disturbed by a first Santonian–Campanian compressional deformation (Guiraud and Bosworth, 1997) and became mostly clastic (Algouti et al., 1999). The Cenozoic Alpine compression (mainly middle–late Eocene to Pleistocene) then inverted the Lower Jurassic normal and transcurrent faults, and folded the EAB (Frizon de Lamotte et al., 2000, 2008, 2011; Hafid, 2000). Offshore in the EAB, salt tectonics are well documented to have been active in Middle Jurassic and Late Cretaceous–Eocene times, with local activity in the Early Cretaceous (Hafid, 2000; Davison et al., 2010; Tari and Jabour, 2013). Brautigam et al. (2009) and Bertotti and Gouiza (2012) mentioned Upper Jurassic–Lower Cretaceous syn-sedimentary tectonics, which they hypothetically related to compressional strain in part of the EAB.

The EAB is presently bounded to the North by the Jebilet High, and to the East and South by the High Atlas (Hafid, 2000) (Fig. 1). The Mesozoic sedimentary strata of the EAB dip gently towards the

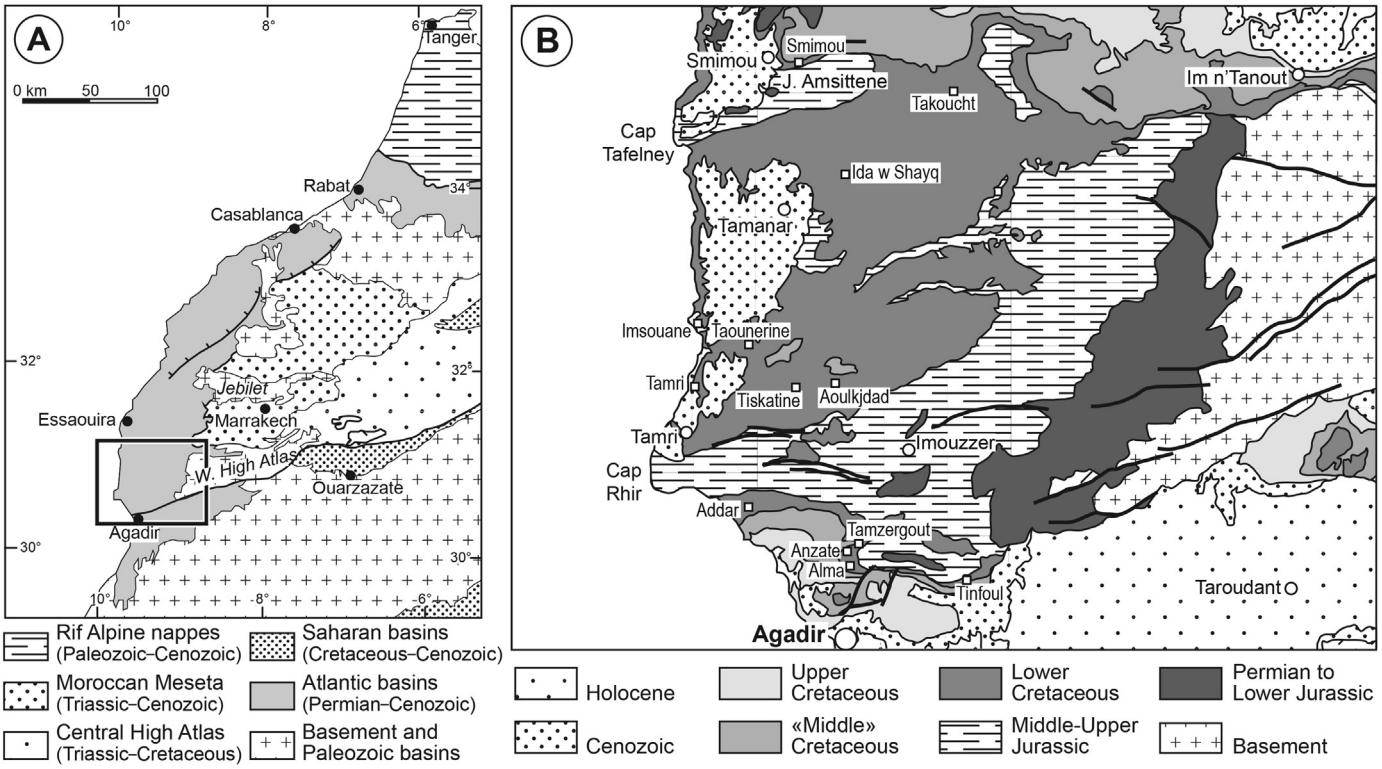

Fig. 1. Location of the study area. A. Location of the Essaouira-Agadir basin. B. Geological sketch of the EAB, and location of the studied sections.

West. The western part of the EAB is divided into three parts by two major E-W trending anticlines, the Amsittene and Imouzzer anticlines, the western tips of which form the Cap Tafelney and the Cap Rhir, respectively (Fig. 1). Between these two major folds, a minor, smooth, E-W trending anticline separates two gentle synclines where Aptian–Albian deposits crop out (Fig. 1B). In the western part of the EAB, uplifted Pliocene marine terraces truncate, and unconformably overlie, the Mesozoic series, and are presently at 50–100 m above sea level.

Most of our present knowledge on the Aptian–Albian stratigraphy is due to Gentil (1905) and Roch (1930), who first described ammonites from this area, to Ambroggi (1963), who proposed an exhaustive stratigraphic scheme for the EAB, based on detailed lithostratigraphic descriptions and associated fossil determination, to Duffaud et al. (1966), who published a synthesis of the area and defined formations in the Cretaceous series, and to Rey et al. (1988), Witam (1998) and Bourgeoini et al. (2002), who conducted micropaleontological studies on the Lower Cretaceous succession. More recently, Peybernès et al. (2013) and Luber et al. (2017; 2019) proposed preliminary stratigraphic, sedimentological and paleoenvironmental analysis of the upper Aptian–lower Albian series of the EAB. According to these authors, the Aptian–lower Albian sedimentary rocks rest on red beds and massive sandstones of the Bouzergoun Formation (Fm.) of late Barremian age, and encompasses (i) the Tamzergout Fm., made of marlstone and limestone of early Aptian age, (ii) the alternating marlstone and limestone of the Tadhart Fm. of early late Aptian age, (iii) the thin, marly Lemgo Fm. of latest Aptian age, and (iv) the mainly marly Oued Tidzi Fm, of early to late Albian age (Fig. 2).

In this work, we shall use the biostratigraphic scheme based on ammonites by one of us (E.R.), which has been published in Peybernès et al. (2013). The study area encompasses the area comprised between the city of Agadir, and the northern major anticline (jebel Amsittene). Thirteen sections of the Aptian–lower Albian series have been studied: five are located south of the Imouzzer anticline, five to the north of the latter, and three at the Amsittene anticline latitude (Fig. 1B, Table 1).

Table 1
Geographical coordinates of the studied sections (see Fig. 1B).

Section	Base	Top
Addar	30°36′04″N – 9°43′31″W	30°35′54″N – 9°43′04″W
Alma	30°31′47″N – 9°35′45″W	30°31′54″N – 9°35′46″W
Anzate	30°32′18″N – 9°35′08″W	30°32′23″N – 9°35′10″W
Aoulkjdad	30°45′47″N – 9°35′31″W	30°46′17″N – 9°35′58″W
Ida w Shayq	31°03′35″N – 9°36′04″W	31°03′31″N – 9°36′01″W
Imsouane	30°50′33″N – 9°48′54″W	
Smimou	31°11′39″N – 9°39′56″W	31°11′42″N – 9°39′56″W
Takoucht	31°09′52″N – 9°24′17″W	31°09′56″N – 9°24′37″W
Tamri	30°45′49″N – 9°48′40″W	30°45′47″N – 9°48′38″W
Tamzergout	30°32′47″N – 9°34′01″W	30°32′40″N – 9°34′12″W
Taounerine	30°48′35″N – 9°44′27″W	30°48′45″N – 9°44′19″W
Tinfoul	30°32′27″N – 9°24′53″W	30°32′24″N – 9°24′58″W
Tiskatine	30°45′43″N – 9°39′14″W	30°46′06″N – 9°39′23″W

3. Material and methods

3.1. Sedimentology and biostratigraphy

Twelve sections have been studied in the central and southern parts of the EAB (Fig. 1B), which are 30–120 m thick, except for the Tamri and Imsouane condensed sections, whose thicknesses do not exceed 20 m. All sections have been measured, studied and sampled bed by bed for paleontological study. Most sedimentological observations have been made in the field, where the lithology, sedimentary features (texture, bioturbation, current figures, dissolution or erosion features etc.), mineral concentrations and faunal assemblages have been carefully noted. Particular attention was paid to the lower and upper bed surfaces, as they bear important information on sedimentary discontinuities.

When present, ammonites were extensively collected bed by bed, and precisely located along the studied section. Ammonites consist of pyritic, phospatic or calcareous molds, the latter being less well preserved. After transport to France, these thousands of ammonites were cleaned and studied by one of us (E.R.), through comparisons with specimens or casts preserved in museum and

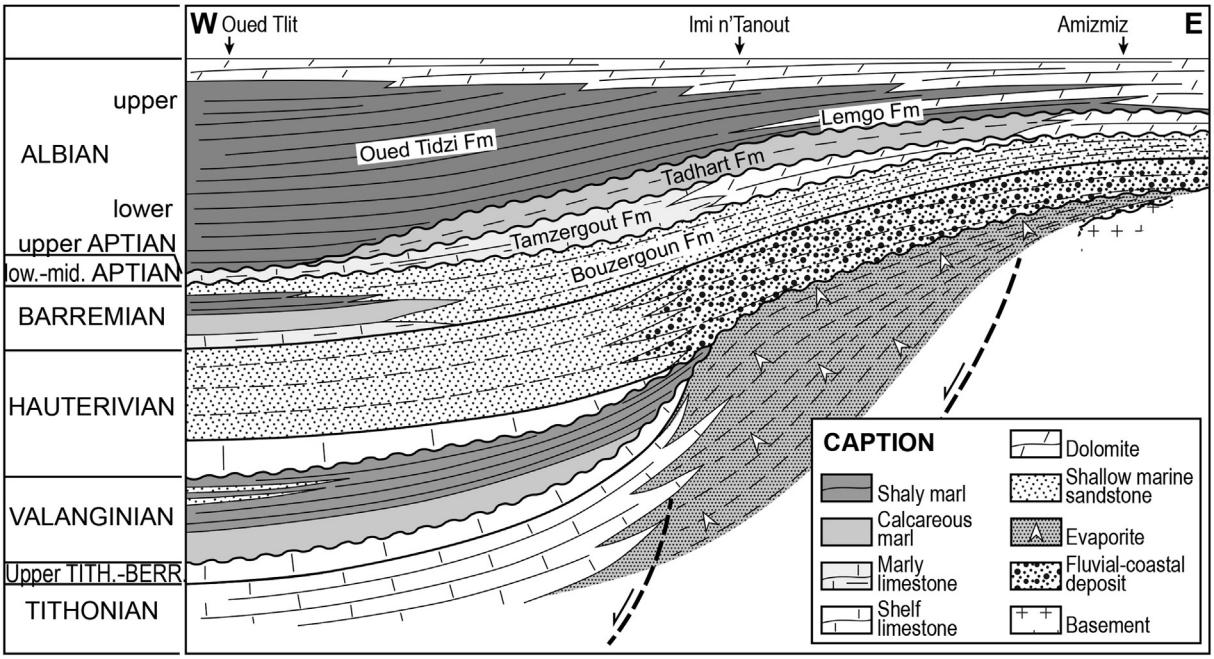

Fig. 2. The Lower Cretaceous deposits in the northern part of the Essaouira-Agadir basin, part of the Atlantic passive margin, from Rey et al. (1988), modified.

university collections, and thanks to the large paleontological collection and library available at the University of Lyon.

3.2. Calcimetry and rock-eval pyrolysis

The calcium carbonate content was measured in 195 samples from five sections (Takoucht, Ida w Shayq, Tiskatine, Anzate and Tinfoul) and in 49 new samples from the Addar, Tamzergout and Alma sections, for which previous results have been published (Peybernes et al., 2013). The calcium carbonate content was determined using the carbonate bomb technique (Müller and Gastner, 1971), which measures CO_2 pressure during a hydrochloric acid attack. For the calculation of the calcium carbonate percentage, see Appendix A in Peybernes et al. (2013).

Twenty-five dark shaly marlstone samples from the Takoucht section were selected for organic matter analysis. Total organic carbon content (TOC), and the nature and thermal maturation of organic matter were estimated using a Rock-Eval 6 Turbo apparatus (Vinci Technologies) at UPMC–University of Paris 6. The method, described in detail by Behar et al. (2001), consists of a two steps analysis with programmed temperature: a pyrolysis between 300 and 650 °C (25°/min), under an inert atmosphere (He), followed by oxidation between 300 and 850 °C (20°/min). All those parameters allow the calculation of the TOC, which is expressed as wt% of bulk rock samples. The hydrogen index (HI), corresponds to the quantity of hydrocarbon compounds released during the pyrolysis relative to the TOC (S2/TOC) in mg of HC per g of TOC, and the Oxygen Index (OI, in mg CO_2/g TOC) is related to the amount of oxygen in the kerogen and is normalized to the S3 value (S3/TOC). Although the source of organic matter is usually defined by the mean of elemental analysis, the HI and OI parameters approximate respectively the H/C and O/C atomic ratios, which are the determining factor for organic matter characterization. The production index (PI) shows the level of thermal maturation. Tmax (°C) is defined as the pyrolysis temperature at which the maximum amount of hydrocarbons is yielded by kerogen. Tmax increases linearly with the natural maturation degree of the organic matter, thus giving a rapid estimate of the thermal maturity of sedimentary basins (Espitalié et al., 1985–1986; Dellisanti et al., 2010). The measurement accuracy is of ±0.05% for TOC, ±2 °C for Tmax, and ±10 for HI and OI. Values are reported in the Appendix.

3.3. Calcareous nannofossils

Calcareous nannofossils were studied in 139 samples from Ida w Shayq, Tiskatine, Anzate and Tinfoul sections. Samples were prepared using the random settling technique of Geisen et al. (1999), adapted from Beaufort (1991), which allows the calculation of absolute abundances (number of specimens per gram of rock). Nannofossils were observed at 1560× magnification using a polarizing light microscope. At least 300 specimens per sample, both coccoliths and nannoliths, were generally counted in a variable number of fields of view (a mean of 446, 369, 402, and 497 for the Anzate, Ida w Shayq, Tinfoul and Tiskatine sections, respectively). An amount of 300 counted specimens is generally considered to be sufficient to have a good estimation of species richness in one sample; in addition, the number of fields of view required to count 300 specimens allows an estimation of the nannofossil abundance (Bown and Young, 1998). In 20 samples (9, 5, 3, and 3 samples from Anzate, Ida w Shayq, Tinfoul and Tiskatine, respectively), less than 300 nannofossils (from 1 up to 208 specimens) were counted, due to the paucity and poor preservation of nannofossils. All nannofossils with at least more than half of the specimen preserved were counted. Both nannofossil total absolute abundance and relative abundances of some key taxa were calculated for each sample. In these calculations, *Nannoconus* spp. were excluded from the total sum of nannofossils because of their uncertain biological affinity (Aubry et al., 2005). The taxonomic frameworks of Perch-Nielsen (1985) and Burnett et al. (in Bown, 1998) were followed. The nannofossil preservation was evaluated following the classes defined by Roth (1983).

Calcareous nannofossils are used in this study to better constrain the paleoenvironmental conditions, in particular, trophic levels in the water column, pelagic carbonate production and sea-surface temperatures. Calcareous nannofossil primary productivity is an indicator of trophic levels in the water column; it is estimated here both with total absolute abundance and relative abundances of fertility indicators such as *Biscutum* spp., *Discorhabdus rotatorius*, *Lithraphidites carniolensis* and small *Zeugrhabdotus* spp. (Table 2; Peybernes et al., 2013). The relative abundances of both *Nannoconus* spp., which constitute the biggest nannofossil carbonate calcifiers and of calcareous nannofossil sea-surface temperature indicators were calculated. Calcareous nannofossils considered as high latitude taxa (*Crucibiscutum* spp., *Repagulum parvidentatum*, *Rhagodiscus angustus* and *Seribiscutum* spp.; Table 2) were considered in this study.

4. Results

4.1. Ammonite biostratigraphy

In the EAB, Aptian and Albian ammonites have been first reported by Brives (1905), Gentil (1905), Lemoine (1905), Kilian and Gentil (1906, 1907) and Roch (1930). While carrying out a regional stratigraphic synthesis of the EAB, Ambroggi (1963) listed Cretaceous ammonite specimens, collected unit by unit and identified by Breistroffer (e.g., Ambroggi and Breistroffer, 1959). Later, Wiedmann et al. (1978, 1982), Rey et al. (1986, 1988), Andreu (1989) and Witam (1998) brought new precisions on ammonite occurrences. Since then, E. Robert (*in* Peybernès et al., 2013) and L. Bulot (*in* Luber et al., 2017, 2019) refined the ammonite biostratigraphy of the Aptian–lower Albian succession of the EAB.

In this work, since many new species and genus have been identified, and the lower part of the successions is locally highly condensed, the presented biozones are accurate but preliminary, pending on careful taxonomic revision (Giraud, Robert et al., in progress). In spite of the absence in our collected samples of many of the zonal markers, we were able to correlate the ammonite successions of the EAB with those of the Mediterranean and Tethyan regions, and thus with the standard biostratigraphic ammonite zones (Reboulet et al., 2018). Although latest Barremian ammonites are present (Jaillard et al., 2019), earliest Aptian specimens from the *Deshayesites oglanlensis* Zone have not been found in the recently studied Aoulkjdad and Takoucht sections, confirming a hiatus of this interval (Peybernes et al., 2013; Luber et al., 2017).

The lower Aptian record is poorly represented, and was best studied in the northern sections. There, the *Deshayesites forbesi* Zone has been tentatively identified by the presence of *Deshayesites consobrinus*, associated with *Ancyloceras* sp. and first cheloniceratids (*Procheloniceras* sp. and *Cheloniceras* sp.). The *Deshayesites deshayesi* Zone is marked by the occurrence of *Deshayesites deshayesi*, *D. consobrinoides*, *D.* cf. *grandis*, *Pseudohaploceras* sp., numerous cheloniceratids specimens (among which *Prochelonicera* spp., *Cheloniceras cornuelianum*, *C. meyendorfi*) and the *Ancyloceras* genus, among which *A.* cf. *matheronianum*. The subsequent *Dufrenoyia furcata* Zone is identified because of the presence of *Dufrenoyia furcata*, *Australiceras* sp. and *Toxoceratoides emericianum*.

The upper Aptian record is well represented in almost all sections. The *Epicheloniceras martini* Zone is identified by the

Table 2
Paleoecological significance of selected calcareous nannofossil taxa.

Taxa	Surface-water fertility	Paleoceanography
Biscutum constans	High[1,2,3,4,5,6,7,8,9]	
	High, but lower than *Z. erectus*[10,11,12]	
B. ellipticum[a]	High[2]	
	Moderate to high[13]	
Biscutum spp.[b]	Moderate[14]	
Crucibiscutum salebrosum		High latitude[15,16,17]
Discorhabdus rotatorius	High[4,5,18]	
	Moderate[13]	Warm waters[9,24], deep-dweller[21]
Repagulum parvidentatum		High latitude[17,25,26,27,28]
Rhagodiscus angustus		High latitude[27]
Seribiscutum gaultensis		High latitude[29]
S. primitivum		High latitude[1,2,3,16,17,27,28]
Zeugrhabdotus erectus	High[1,2,3,6,7,10]	
small Zeugrhabdotus (with major axis ≤5 mm)	High[7,8,11]	

1. Roth (1981); 2. Roth and Bowdler (1981); 3. Roth and Krumbach (1986); 4. Erba (1987); 5. Premoli Silva et al. (1989); 6. Roth (1989); 7. Watkins (1989); 8. Williams and Bralower (1995); 9. Mutterlose and Kessels (2000); 10. Erba (1992); 11. Erba et al. (1992); 12. Eleson and Bralower (2005); 13. Giraud et al. (2003); 14. Linnert et al. (2010); 15. Mutterlose (1992a); 16. Mutterlose (1992b); 17. Street and Bown (2000); 18. Coccioni et al. (1992); 19. Tappan (1980); 20. Busson and Noël (1991); 21. Erba (1994); 22. Pauly et al. (2012); 23. Scarparo Cunha and Shimabukuro (1997); 24. Mutterlose (1989); 25. Wise (1988); 26. Erba et al. (1989); 27. Crux (1991); 28. Watkins et al. (1996); 29. Lees (2002).

[a] *B. ellipticum* is considered as a morphotype of *B. constans* (Bornemann and Mutterlose, 2006).

[b] *Biscutum* spp.: *B. constans* (abundant), *B. ellipticum* (common) (Linnert et al., 2010).

appearance of numerous specimens of the *Epicheloniceras* genus (*E. martini*, *E. tschernyschewi*), together with *Colombiceras crassicostatum* and other species of the genera *Vectisites*, *Neodufrenoyia* gen. nov. and *Colombiceras*. The upper part of the *E. martini* Zone is marked by a well correlatable horizon bearing abundant *Australiceras* and *Pseudoaustraliceras* ("Tropaeum beds" of the literature).

The *Parahoplites melchioris* Zone is poorly represented in the EAB. The association of *Acanthohoplites* sp., *Colombiceras discoidales* and *Valdedorsella akuschaense* is tentatively ascribed to this zone. In overlying strata, the *Acanthohoplites nolani* Zone and subsequent zones present a fairly high faunal diversity.

The *Acanthohoplites nolani* Zone is represented in all sections and the historical, long recognized "nolani bed" represents a good correlation level. Bulot and Latil (2014) called into question the use of *A. nolani* as a zone index, and Luber et al. (2017) pointed out the misidentification of this species for the Moroccan representatives, and introduced the species *Esaisabellia tiskatinensis*. Nevertheless, we will follow the current standard zonation, awaiting for next discussions of this purpose by the Kilian Group. In the "*A. nolani*" zone, the associated fauna consists of *Epicheloniceras clansayense*, *Aconeceras aptiana*, *Pseudohaploceras* sp., *Diadochoceras* sp., *Zuercherella* sp. and specimens of the *Neodufrenoyia* gen. nov. and *Acanthohoplites* genera (among which *A. bergeroni*, *A. bigoureti anthulai*).

The *Hypacanthoplites jacobi* Zone is mainly represented by pyritous ammonites, and is defined by the first occurrence of *Hypacanthoplites* spp. (*H. nolaniformis*, *H. elegans*, *H. clavatus*). They are associated with *Epicheloniceras clansayense*, *Pseudorbulites convergens*, *Phylloceras (Phylloceras) aptiense*, *Diadochoceras migneni*, *Parasilesites kilianiformis*, and representatives of the genera *Eogaudryoceras*, *Fallotermiericeras* gen. nov., *Neodufrenoyia*, first *Phyllopachyceras* and *Eogaudryceras (Eotetragonites)*.

The lowermost Albian record is well represented, although the corresponding fauna is poorly preserved. The *Leymeriella tardefurcata* Zone is characterized by the occurrence of various specimens of Silesitoidinae and of the genera *Phylloceras*, *Phyllopachyceras*, *Hypacanthoplites*, *Mellegueiceras*, *Parengonoceras, Uhligella, Pusozia*, *Eogaudryceras (Eotetragonites)* together with *Douvilleiceras leightonense*, *Oxytropidoceras (Oxytropidoceras)* sp., *O. (Mirapelia) mirapelianum, Neosilesites palmensis, Ptychoceras laeve, Parabrancoceras* sp. and other less representative or endemic specimens. Mainly because of poor outcrops in a chiefly argillaceous series, the *Douvilleiceras mammillatum* Superzone is less represented. However, the occurrence, among others, of *Douvilleiceras mammillatum aequinodum*, *Prolyelliceras gevreyi*, *Beudanticeras dupinianum africana*, *B. revoili*, *Uhligella rebouli*, *Parengonoceras bussoni* and *P. hachourii* characterizes this time span. The "Beudanticeras beds" (Roch, 1930; Ambroggi, 1963) mostly belong to this interval.

Toward the West (Tamri, Imsouane), the Aptian–lower Albian series is condensed in a phosphate- and glauconite-rich, conglomeratic level, which contains ammonites of early Aptian to earliest Albian age (Robert, *in* Peybernès et al., 2013).

4.2. Sedimentary facies

Aptian facies differ from those of the uppermost Aptian–lower Albian series, in their lithology and detrital quartz content, as well as in their faunal content.

4.2.1. Aptian facies (Fig. 3)

Facies 1 (F 1): Facies 1 is made of shales or shaly marlstone, containing mainly belemnites and some ammonites. Sandstone or marl beds are almost absent (less than 5% in thickness). Scarce thin-shelled bivalves, annelids (serpulids) and small-sized gastropods may occur. Because of the shaly nature of the deposits, bioturbation is hardly visible. Ammonites may be pyritous.

Interpretation: The lack or scarcity of carbonate suggests that sedimentation took place far from the "carbonate factory" (Tucker and Wright, 1990; Schlager, 2003) located in the nearshore euphotic zone, where photosynthesis favours the organic activity of carbonate generating organisms (from bacterias to algae and molluscs). The strong predominance of pelagic organisms and the scarcity of benthic fauna suggests a deposition below the euphotic zone. Therefore, facies F1 is interpreted as characterizing distal outer shelf deposits.

Facies 2 (F 2): Facies 2 consists of shales or shaly marlstone, with some marly beds (about 20–30% of total thickness). The faunal content is dominated by belemnites, ammonites, irregular sea urchins, brachiopods (terebratulids) and plicatulids, associated with some gastropods, bivalves (mostly thin-shelled), annelids and scarce nautiloids. Isolated corals locally occur. Bioturbation consists of track molds, small sized curved burrows and digging traces (sediment feeders), mainly visible in the marlstone beds.

Interpretation: The occurrence of benthic, relatively deep water organisms (e.g. echinoids, brachiopods), together with planktonic fauna (cephalopods) suggests a hemipelagic environment. The lithological association (prevailing marl, subordinate limestone) also points to an outer shelf setting. Bioturbation is dominated by the activity of sediment feeders, suggesting an outer shelf environment and moderately oxygenated conditions.

Facies 3 (F 3): Facies 3 is made of marly limestones (about 30–50% of total thickness) with marly interbeds. The faunal content is dominated by benthic organisms, such as brachiopods, annelids and bivalves, among which oysters, plicatulids, pectinids and thick-shelled large bivalves. Ammonites occur commonly. Bioturbation dominantly consists of burrows (curved and straight) and track molds.

Interpretation: The predominance of a diversified benthic fauna indicates a shallow, open marine environment, while the abundance of limestone suggest the proximity of the "carbonate factory" and hence, of a carbonate platform. However, the lack of algae and of very shallow organisms or features (e.g. oncolites, rudistids, corals) precludes a very shallow environment. The dominance of burrows and surficial track molds supports the interpretation of a shallow (proximal) open shelf environment.

Facies 4 (F 4): This facies is lithologically marked by thick, massive limestone beds, containing shallow marine benthic bivalves, such as abundant oysters, some trigonids and scarce rudistids. Bioclasts are common and belemnites may occur at the top of these beds. Bioturbation is represented by burrows. The top of these beds is locally karstified (see surface S1, below).

Interpretation: The predominance of a shallow marine benthic fauna indicates a shallow carbonate shelf environment. Evidence of frequent emergence at the top of these deposits support this interpretation. The presence of bioclasts suggests a moderate energy environment, which is supported by the predominance of suspension feeders. F4 sediments are thus interpreted as deposited in a well oxygenated, shallow to very shallow carbonate shelf environment, with moderate energy.

4.2.2. Uppermost Aptian–Albian facies (Fig. 3)

Facies I (F I): Facies I is made up of monotonous, dark-coloured, almost azoic shales or shaly marlstones. Long searches on these outcrops allowed only to find scarce ammonite casts.

Interpretation: The lack of fauna and sedimentary structures makes any reliable interpretation difficult. However, as this facies usually overlies or underlies the FII facies, is devoid of benthic fauna, and occurs at the top of the studied sections, it is interpreted as a pelagic, deep water marine deposit.

Facies II (F II): Facies II is very comparable to the F 1 facies, and consists of silty shales or silty shaly marlstone, containing mainly belemnites and some ammonites. Sandstone beds are virtually absent (less than 5% of the total thickness). Scarce thin-shelled bivalves, annelids, plicatulids, small sized gastropods and brachiopods (mostly rynchonellids) occur sporadically. Because of the shaly nature of the deposits, bioturbation seems to be absent, except in the sandstone or marlstone beds, where digging tracks dominate.

Interpretation: The lack, or scarcity, of carbonate suggests that sedimentation took place far from the carbonate factory, i.e. in a distal place, if the carbonate content is due to export from shallow water deposits. The strong predominance of pelagic organisms and the scarcity of benthic fauna support a deposition depth below or near the lower limit of the euphotic zone. Therefore, facies F II is interpreted as a hemipelagic deposit, in a distal outer shelf environment, and is thought to be roughly equivalent to the F 1 facies.

Facies III (F III): Facies III is made of shales or shaly marls, with thin beds of sandstone or sandy marl (about 30% of the total thickness). The faunal content is dominated by belemnites, ammonites and brachiopods (mostly terebratulids), associated with some gastropods, plicatulids, and thin-shelled bivalves. Bioturbation in the sandstone beds consists of small sized curved burrows and digging traces (sediment feeders).

Interpretation: The occurrence of benthic, relatively deep water organisms (e.g. brachiopods, plicatulids), together with planktonic fauna (cephalopods) suggests a hemipelagic environment. The lithological association (prevailing silty to sandy marlstone) also points to an outer shelf setting, comparable to that of Facies F 2. However, the presence of sediment feeders, even in the sandstone beds, suggests that sea bottom waters were less oxygenated than in Facies 2.

Facies IV (F IV): F IV consists of yellow, dolomitic, well-sorted sandstone beds, usually separated by silty to marly interbeds. The faunal content is dominated by benthic organisms, such as brachiopods (terebratulids) and bivalves, among which gastropods, oysters, plicatulids, pectinids and other bivalve fragments. Ammonites and belemnite fragments are common. Sedimentary structures such as current ripples and cross-bedding are also common. The lower part of the dolomitic sandstone beds is commonly rich in varied reworked elements: phosphatic fragments, internal molds of gastropods or ammonites, brachiopods, lithoclasts and belemnite rostra. Bioturbation consists of burrows (curved and straight), track molds and digging traces. F IV commonly overlies erosional surfaces, below described as S 4.

Interpretation: The predominance of a diversified benthic fauna indicates an open marine environment. The occurrence of current-related structures indicates a moderate to high energy during deposition, which is supported by the good sorting of sandstone grains. The abundance and diversity of bioturbation, as well as the energetic conditions, support the interpretation of a shallow (proximal) outer shelf environment, probably above the fair-weather wave base. When F IV deposits overly S 4 surfaces, they are interpreted as resulting from the decreasing intensity of submarine currents responsible for the erosional surface. As these currents decrease, they allow deposition of sandstones, mixed with reworked elements, both brought out from the underlying, eroded strata. When F IV does not overly S 4 surfaces, it may be interpreted as storm deposits, resulting from an abrupt detrital supply derived from littoral areas, possibly related to river floods, or resulting from high frequency relative sea-level drops.

Facies D (F D): Facies F D is characterized by a poor faunal diversity, together with the high abundance of one type of organism, usually annelids (serpulids) or buchidae bivalves (e.g. *Aucellina* sp.). F D is usually associated with monotonous shales or shaly marlstones, or with alternating marlstone/silty marlstone and marlstone/sandstone, with predominance of marlstones or silty marlstones (lithologies of F 1, F 2, F II or F III). Bioturbation is sparse, but this may be due to the shaly lithology. Pyrite is commonly abundant.

Interpretation: The poor faunal diversity, the presence of pyrite and the predominance of organisms tolerating oxygen-depleted environments (buchidae, serpulids, De la Mora et al., 2000; Henderson, 2004) point to dysaerobic conditions. However, the occurrence of scarce bioturbation indicates that benthic life was still possible, and therefore, that conditions were not anoxic. Because of the scarcity of other fauna, the depositional environment is difficult to assess precisely, and it will be interpreted based on the lithology. For this reason, the dysaerobic facies (F D) will be named based on their lithology, for instance F 2D or F IID. In all

cases, in the studied sections, F D is of restricted to outer shelf environments.

4.3. Peculiar sedimentary surfaces

Surface 1 (S 1): The first type of surface is usually found on top of a massive limestone bed. It is an uneven, corroded surface, the cavities of which are filled by the overlying highly glauconitic deposits, or by iron oxydes (see below) (Fig. 4A,B). The centimeter-scale cavities may penetrate in the limestone beds as much as several tens of centimeters deep. In the upper surface of the bed, the calcite of bioclasts has been locally dissolved and is replaced by iron oxydes, iron-rich dolomite or by glauconitic-rich sediments.

Interpretation: S1 is interpreted as a karstified surface, which indicates a period of subaerial exposure and explains the dissolution by meteoric water. S1 is, therefore, interpreted as a sequence boundary (SB). It is only found at the base of the studied sections (i.e. in lower Aptian deposits), and mainly in the southern part of the basin, where several S 1 surfaces may be amalgamated. In the latter case, reworked ammonites of different ages suggest large time gaps.

Surface 2 (S 2): The second type of surface is represented by a thin layer of highly glauconitic, sometimes phosphatic deposits that commonly form a crust. It commonly contains lithoclasts, fossils and bioclasts (oysters, brachiopods, gastropods, belemnites, ammonites) of various nature and origin. It may fill the karstic cavities and depressions of S1, or form a distinct layer. In some cases, large lithoclasts are bored (Fig. 4C).

Interpretation: S 2 is thought to represent a condensed deposit, resulting from a submarine hiatus. The occurrence of a variety of organisms living in shallow to moderately deep environments suggests that condensation partly occurred in a shallow marine environment. This is supported by the local presence of bored clasts, boring being restricted to shallow marine environments and being common in tidal environments. However, the presence of glauconite and phosphate suggests that at least part of the condensation occurred in an outer shelf environment, likely related to mineralised, deep water currents. S 2 is, therefore, interpreted as related to a transgressive episode. S 2 is usually found at the base or at the top of the studied sections, and only in the western part of the basin.

Surface 3 (S 3): Surface 3 is marked by a thin, discontinuous, iron-rich crust, which covers the upper surface of marly or calcareous beds (Fig. 4D). It is locally associated with some small-sized lithoclasts, and concentrations of pelagic fauna (cephalopods). It is mainly recorded in the upper Aptian deposits.

Interpretation: S 3 is interpreted as a hard ground representing a submarine hiatus, likely related to marine currents. In upper Aptian deposits, S 3 commonly laterally evolves to S 4 surface (submarine erosion, see below). In this case, S 3 is interpreted as resulting from the mineralization by submarine currents of a hard bed (calcareous marlstone or limestone) that resisted to the submarine erosion, the latter having removed the underlying shales and being still active elsewhere. In the western, condensed sections, S 3 may be merged with S 1 or S 2 surfaces.

Surface 4 (S 4): An other type of surface is found at the base of high concentrations of belemnites rostra associated with lithoclasts, flat pebbles, phosphatized white internal molds of fossils (commonly gastropods and ammonites) and scarce other bioclasts (Fig. 4E and F). These elements can be found, either as coquina layers within a marly shale succession (S 4A), or reworked at the base of, or within, limestone or calcareous

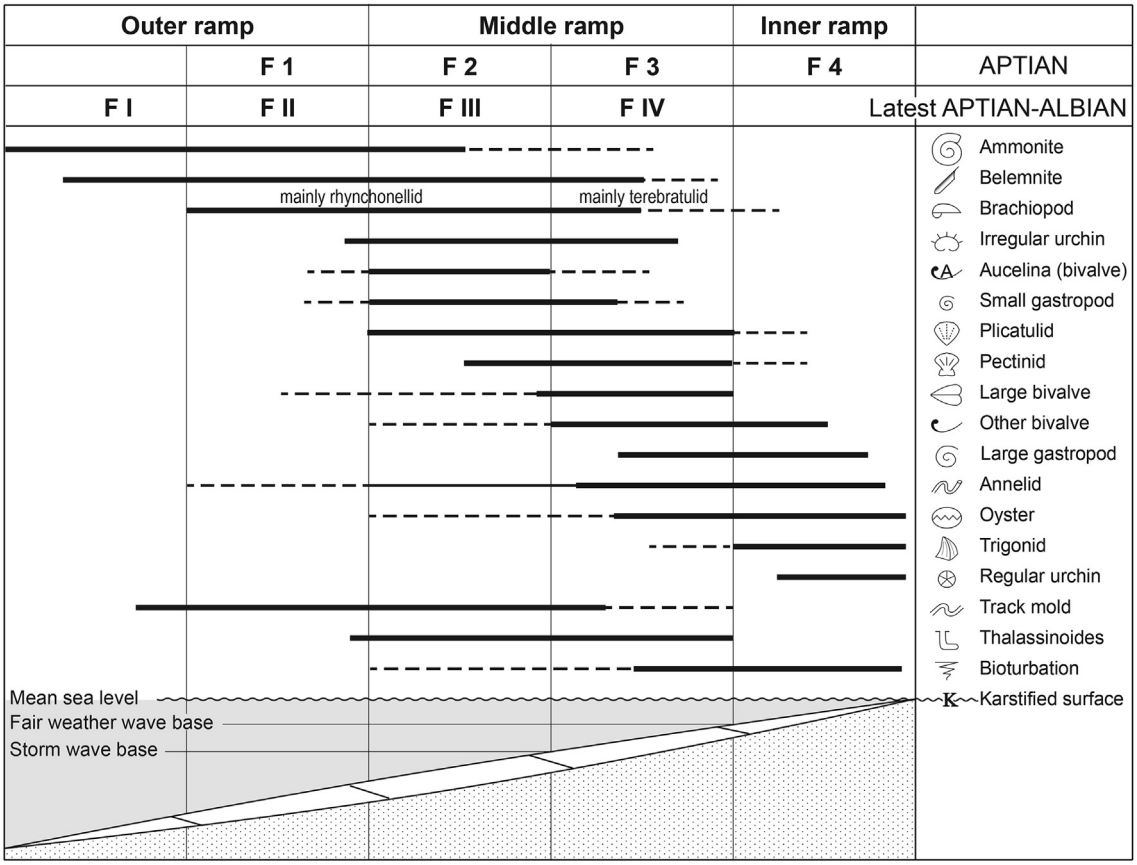

Fig. 3. Sedimentary facies of the Aptian (A) and uppermost Aptian–Lower Albian (B) along the ramp of the Essaouira-Agadir basin.

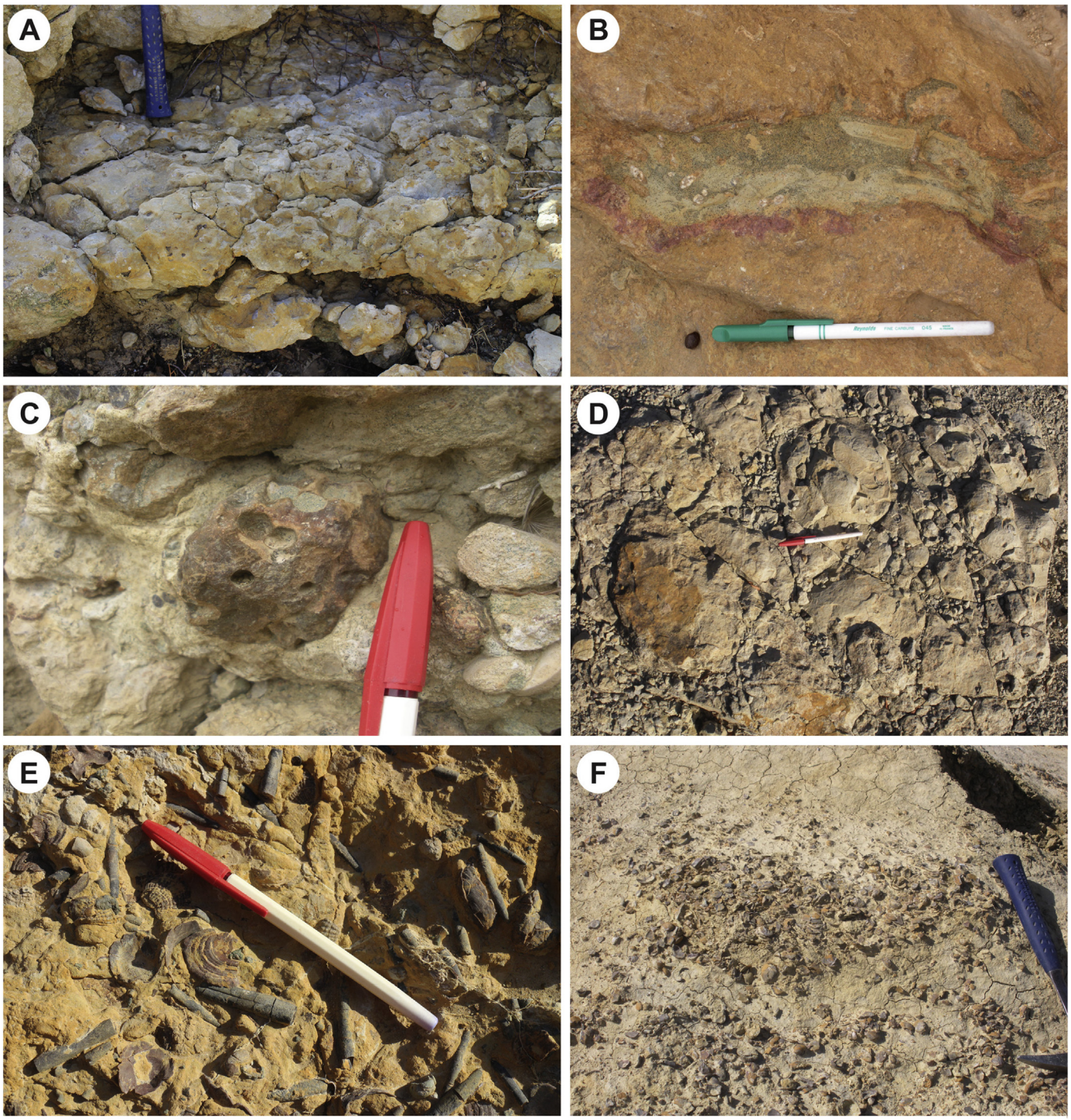

Fig. 4. Types of sedimentary surfaces in the Essaouira-Agadir basin. A. Karsted surface S1 (D1, Takoucht section). B. Glauconitic infilling of a karstic cavity on a S1 surface (D1, Addar section). C. Bored rounded clast in a phosphatic conglomerate (S2 surface, Tamri section). D. Iron oxide rich crust (S3 surface, D3, Addar section). E. Concentration of belemnites and plicatulids and gastropod shells at the base of a dolomitic sandstone bed (S4B surface) (D4, Taounerine section). F. S4A surface marked by a concentration of brachiopods and plicatulids shells in a marly succession (D4, Ida w Shayq section).

sandstone beds (S 4B) (see Fig. 5). In the first case (S 4A; Fig. 4F, and D4 in Ida w Shayq section on Fig. 5), these coquinas are frequently lenticular in shape, since they overlie a slightly uneven surface, and may be associated with fine-grained sand. Where the coquina is lacking, S 4 may be only marked by a slight lithological change, associated with an upward change in the faunal content, from pelagic organisms to assemblages including benthic species. In the second case (S 4B; Fig. 4E), clasts, bioclasts and molds are concentrated at the base of the overlying bed, and rapidly disappear upward. S 4 occurs in the uppermost Aptian and lower Albian succession.

Interpretation: S 4 may be interpreted in two distinct ways. In the most common case, the reworked faunal assemblage, as well as the overlying one, contain pelagic organisms. Such an erosional

surface is interpreted as representing a submarine hiatus, associated with erosion of the underlying marlstone or shale, related to relatively strong submarine currents. In this interpretation, the submarine erosion would have removed the small-sized sedimentary particles (shale, marlstone), thus bringing out and concentrating their detrital and pelagic faunal content. The frequent occurrence of phosphatic internal molds of organisms suggests that upwelling currents played a role in this erosion and allowed phosphatisation of carbonate elements during the erosional hiatus. However, since the S 4 surface is always found at the top of shaly or marly series, the occurrence of emersion periods cannot be ruled out for some of these surfaces. As a matter of fact, on one hand, the overlying bed may contain shallow water fauna (oysters, trigonids, corals), and on the other hand, shale or marlstone cannot be karstified, and possible evidences of subaerial erosion (e.g. paleosoils, fluvial or eolian sands, etc.) may have been eroded, and removed or reworked by the overlying, transgressive high-energy deposits.

4.4. Calcimetry and rock-eval pyrolysis

For all successions, calcium carbonate values are higher in the Aptian than in the Albian deposits, with values generally comprised between 40% and 90% up to the end of the *A. nolani* ammonite Zone. Close to the Aptian–Albian boundary, the calcium carbonate content sharply decreases, and remains low or slightly decreases through early Albian times (Fig. 6).

In the Takoucht section, the 25 analyzed samples contain between 0.2 and 1.5% TOC, with an average of 0.7%. There is no clear relationship between TOC% and $CaCO_3$% (Fig. 6), which suggests that the percentage of organic matter does not result from its dilution by carbonate input. Hydrogen indices are comprised between 128 and 198 mg/g of rock, Oxygen indices from 159 to 311 mg/g, S1 from 0.01 to 0.05 mg/g, and S2 from 0.12 to 3.01 mg/g. The PI is always very low with values in the range of 0.01–0.16. Temperatures of maximum pyrolytic yield (Tmax) are in average of 438 °C (Appendix), indicating that the organic matter did not experience high temperature during burial. Thus, organic matter in the Takoucht section was still immature with respect to petroleum generation. The very low free hydrocarbon content (S1 = 0.01–0.05 mg/g rock) confirms this immaturity. Such low maturation allowed the use of the hydrogen index (HI) as an indicator of the origin and composition of the organic matter (Espitalié et al., 1985–1986). According to the low range of the HI values, the organic matter of the Takoucht section could be attributed to Type III, related to terrestrial higher plants debris or to altered Type II, derived mainly from algae and/or bacteria, but highly oxidized.

4.5. Calcareous nannofossils

Calcareous nannofossil total absolute abundance, relative abundances of calcareous nannofossil fertility (meso-eutrophic taxa), sea-surface temperature indicators (cold taxa) and *Nannoconus* spp. are plotted with the ammonite biostratigraphic information for each section. Calcareous nannofossil data obtained from the present study (Ida w Shayq, Tiskatine, Anzate and Tinfoul) are compared to those published from Addar, Tamzergout and Alma (Peybernès et al., 2013) (Figs. 6 and 7). The lower part of the Alma succession contains many barren samples due to dolomitization. This section is not shown in Fig. 7, because the few scattered data do no allow to comment any trend.

In the studied sections, preservation of calcareous nannofossils is poor to good and fluctuates all along the successions (Fig. 7); some samples of both Tiskatine and Anzate sections are barren of nannofossils and/or contain very rare nannofossils (Fig. 7). The means of the nannofossil total absolute abundance are higher in the distal sections of Addar (0.57×10^9 specimens per gram of rock), Ida w Shayq (0.43×10^9), Tiskatine (0.35×10^9) and Tamzergout (0.33×10^9), with respect to the more proximal sections of Anzate (0.18×10^9) and Tinfoul (0.13×10^9). A progressive decrease in the nannofossil total absolute abundance is recorded through the Aptian–lower Albian interval, except for the Ida w Shayq section, which shows a sharp decrease around the Aptian–Albian boundary (Fig. 7). The mean relative abundance of meso-eutrophic taxa is comprised between 17.8 (Ida w Shayq) and 28.6% (Addar), which represent relatively high values. The relative abundance of meso-eutrophic taxa follows an opposite trend with respect to the nannofossil total absolute abundance, since it generally increases in the uppermost Aptian and lowermost Albian (between D3 and D5); in both Tamzergout and Anzate the absence of data below this interval does not allow to observe this trend (Fig. 7). Above D5 (*D. mammillatum* Superzone), the relative abundance of meso-eutrophic taxa decreases (Fig. 7). In all sections except Tinfoul, an increase in the relative abundance of cold taxa is recorded from the upper Aptian to the lower Albian, and the Anzate section shows higher percentages than the other ones (Fig. 7). The relative abundance of the largest nannofossil calcifier, *Nannoconus* spp., decreases from the upper Aptian to the lower Albian (Fig. 7). The proximal Tinfoul section presents both the lowest *Nannoconus* spp. percentages and calcium carbonate contents (Fig. 6).

5. Interpretations

5.1. Aptian–lower Albian depositional sequences

The identification of facies and discontinuity surfaces allowed us to define eight depositional sequences in the Aptian–lower Albian interval (≈15 Ma).

The **first sequence** (<10 m) is only developed in the northern part of the EAB. In Ida w Shayq and Smimou, its lower part yielded latest Barremian ammonites (*M. sarasini* ammonite Zone, Jaillard et al., 2019), whereas the upper part contains ammonites from the *D. deshayesi* Zone at Smimou, Ida w Shayq and Aoulkjedad. Its lower limit (D 0, Figs. 5, 8–10) is an S 1-type, karstified surface. At Ida w Shayq, parts of the section are covered, and it is possible that this sequence includes an additional, unobserved discontinuity. The lower, transgressive part of the sequence is dominated by marlstone and sandstone beds rich in oysters, with subordinate pectinids and trigonids. The middle part contains irregular urchins, associated with ammonites, oysters and serpulids, while the marly to calcareous upper part yielded mainly ammonites and brachipods. Its top is usually represented by a remarkable accumulation of cheloniceratids (« *Cheloniceras* bed »), locally exhibiting karstic dissolution (Ida w Shayq). These features indicate an overall transgressive trend for the sequence. In the southern sections, this sequence may be represented by the undated infilling of karstic cavities related to amalgamated emersion surfaces. This sequence seems to roughly coincide with the Tamzergout Fm of Rey et al. (1988) and Witam (1998).

The **second sequence** (<11 m) is mainly observed in the northern part of the basin. In the Ida w Shayq section, it yielded late early to early late Aptian ammonites (*D. deshayesi ?* to *E. martini* zones). Its lower boundary (D 1, Figs. 5, 8–10) is an S 1 surface in Takoucht, Ida w Shayq and Aoulkjdad. There, it is marked by a thinning upward succession of limestone beds. Whereas the lower part is dominated by ammonites and brachiopods, the shaly upper part mainly contains plicatulids and scarce ammonites. This evolution is interpreted as a mainly transgressive succession, the regressive part of the second sequence being eroded below the

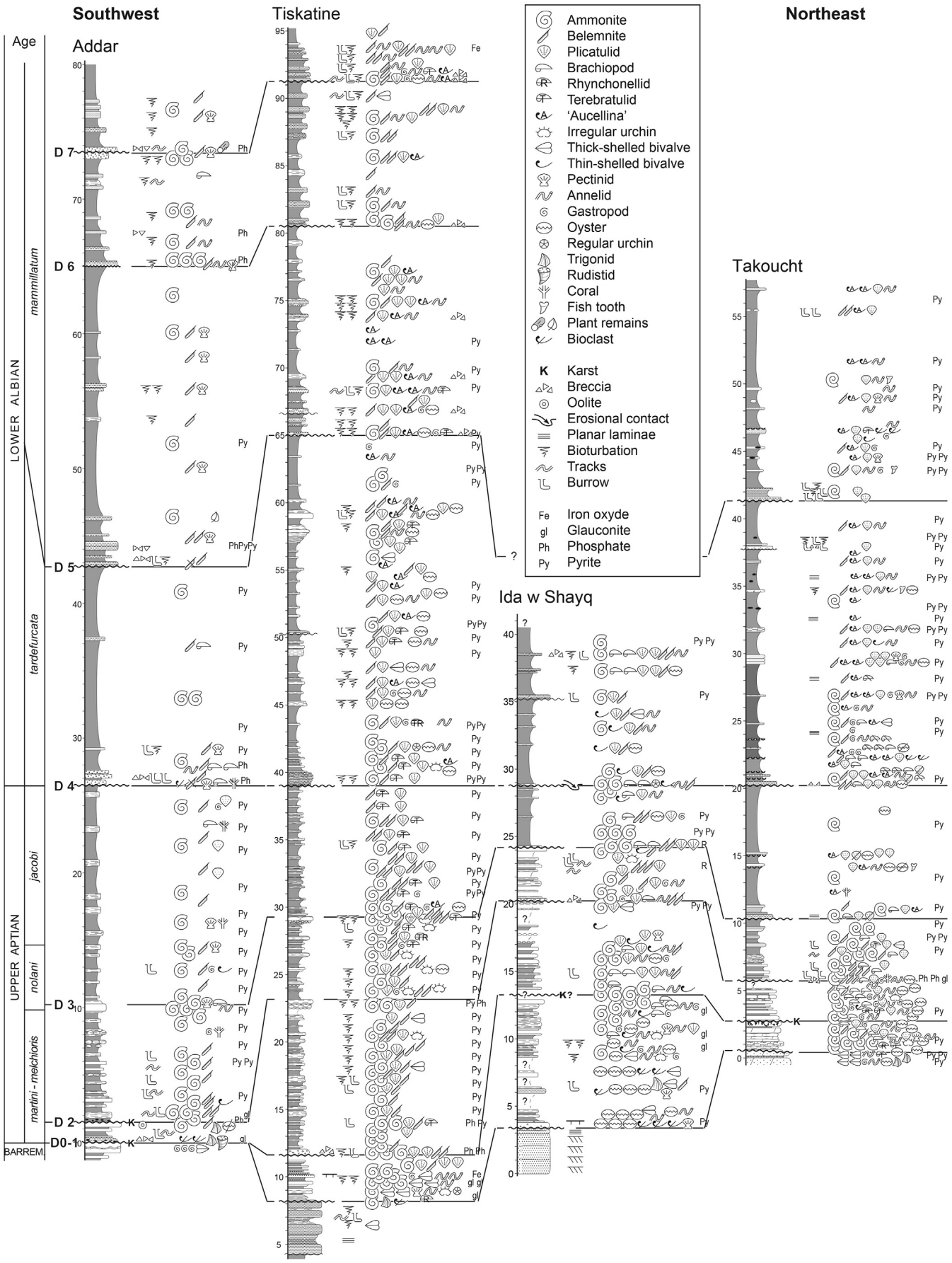

Fig. 5. North-South correlations of some Aptian–lower Albian sections of the Essaouira-Agadir basin.

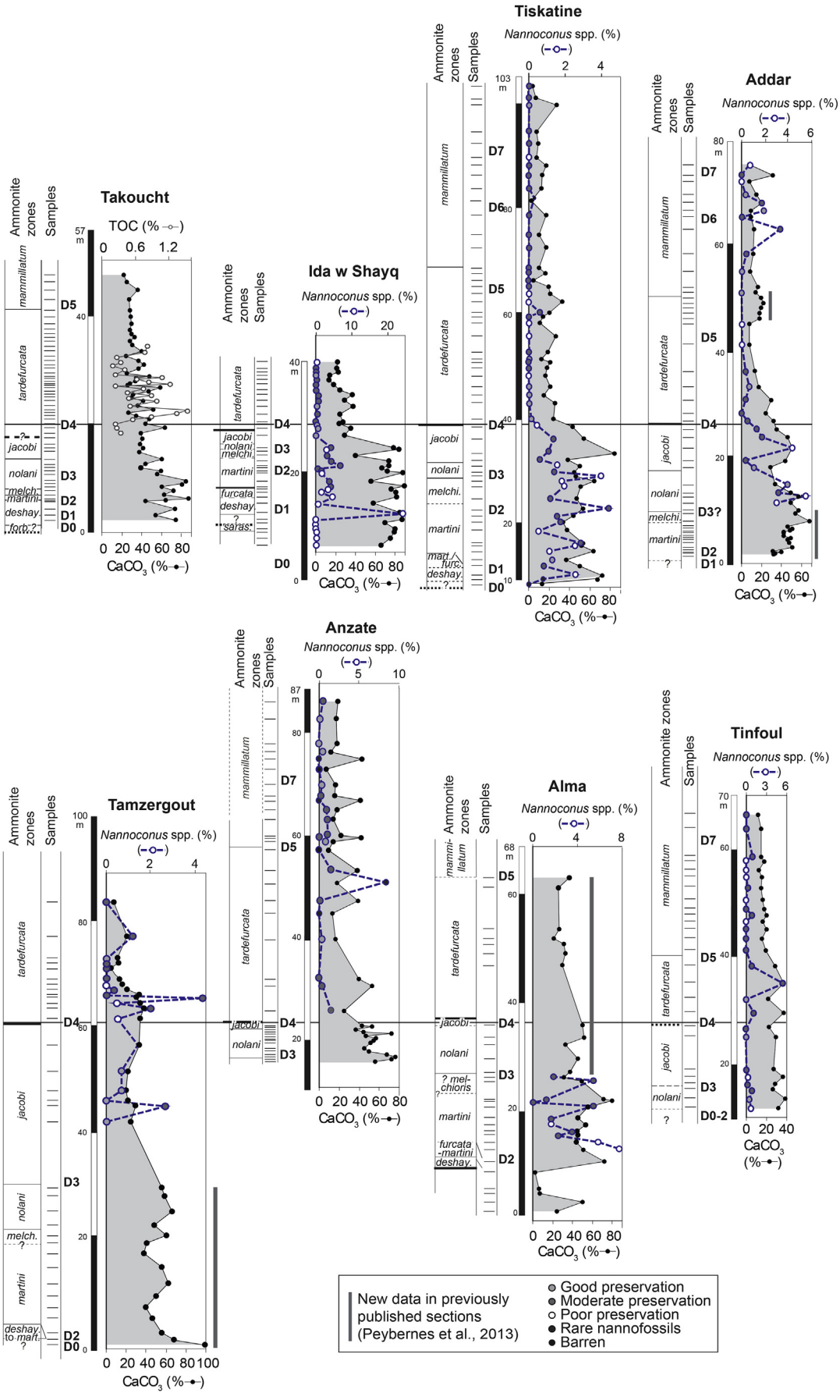

Fig. 6. Stratigraphic changes in calcium carbonate content and relative abundances of *Nannoconus* spp. for the different sections. For the Takoucht section, the TOC is added. The sedimentary discontinuities (D0–D7) are indicated.

upper discontinuity surface. In the Tiskatine and Aoulkjdad sections, it is represented by a monotonous marlstone-limestone alternation, rich in plicatulids, belemnites and ammonites. This sequence commonly ends with a limestone bed rich in large ammonites (« 'Tropaeum' bed »). In the southern sections, the second sequence is usually represented by a massive limestone bed intercalated between two emersion surfaces (S 1), whereas it is lacking in the easternmost section (Tinfoul, Fig. 8).

The **third sequence** (<14 m) is recorded in all sections. It yielded early late Aptian ammonites (*E. martini*, to base of *A. nolani* zones). Its base (D 2, Figs. 5, 8–10) is locally a S 4B surface, consisting of a limestone bed rich in phosphatized fossils (Addar, Ida w Shayq). Elsewhere, the base of the sequence is placed at the top of the "Tropaeum bed" (S 3 surface). This sequence comprises a first thinning-upward, then thickening upward alternation of shaly and calcareous marl beds. The fauna is dominated by belemnites, ammonites and plicatulids, which are associated with oysters at the base, irregular urchins in the middle part, and brachiopods at the top of the sequence. This faunal evolution supports a deepening-, then shallowing-upward trend. In all sections, its top is clearly marked by a noticeable marly limestone bed extremely rich in «*Nolaniceras*» spp. (« Nolani bed »). The second and third sequences appear to correspond to the Tadhart Fm (Rey et al., 1988; Witam, 1998).

The **fourth sequence** (<5–30 m) crops out in all sections. It is well dated by latest Aptian ammonites (*A. nolani* to *H. jacobi* zones). Its base (D 3, Figs. 5, 8–10) is locally marked by a slightly erosional sandy bed (Anzate Alma, Tamzergout, Takoucht). At Aoulkjdad, it consists at the base (S 4B) of a bed rich in phosphatized ammonites and bioclasts. Elsewhere, it is marked by the oxydized top of the « Nolani bed » (S 3). In Takoucht, a low angular unconformity can be seen between the sandstone bed (S 4 surface) and the « Nolani bed » (S 3 surface), thus evidencing submarine erosion, which took place during the hiatus causing the sequence boundary (Fig. 10). The fourth sequence is usually a thinning-upward, mainly marly succession, rich in ammonites, belemnites and plicatulids. According to the sections, thin sandstone beds are present (Addar, Anzate, Taounerine), some ammonites are pyritous (Anzate, Taounerine), and calcareous beds appear in the upper part of the sequence (Ida w Shayq), illustrating a progradational trend. The presence of numerous *Aucellina* sp. and of abundant pyrite suggests reducing conditions, which represent the equivalent of one of the upper Aptian anoxic events known in southeastern France (Kennedy et al., 2014 and references therein). This sequence is correlated with the Lemgo Fm of Rey et al. (1988) and Witam (1998).

In Tamzergout, the Aptian–lower Albian succession is thicker than elsewhere, and the more complete ammonite succession suggests that an additional sequence (12 m) is preserved below the major discontinuity of the Aptian–Albian boundary (D 4′, Fig. 8). If so, this would imply on one hand that subsidence was higher in this area than in other areas, and on the other hand that the overlying unconformity surface is strongly erosive, as this sequence is not recorded elsewhere.

The **fifth sequence** (<35 m) is well represented in all studied sections. It yielded numerous ammonites, which ensure an earliest Albian age (*L. tardefurcata* Zone). The lower sequence boundary (D 4, Figs. 5, 8–10) is a typical S 4B surface at the base of a reworked bed, reflecting strong erosion. Among the reworked bioclasts in the basal sandy bed, the presence of corals (Addar), pectinids (Tamzergout), oysters (Tiskatine, Takoucht) or regular urchins (Ida w Shayq) suggests a shallow marine environment. Therefore, the occurrence of subaerial erosion related to a significant sea-level drop cannot be ruled out for this sequence boundary, which encompasses the Aptian–Albian boundary time-span. An emersion period during D 4 is supported by the fact that sequence 4 is locally deeply eroded, with its thickness varying between 30 m (Tamzergout) and 5 m (Anzate) in the South (Fig. 8), and between 4 m (Aoulkjdad) and 11 m (Taounerine) in the center of the basin (Fig. 9). The fifth sequence is mainly made of shaly marlstone, containing belemnites, ammonites and plicatulids, although oysters, brachiopods, pectinids and annelids may occur as well. This sequence is locally rich in buchidae bivalves (*Aucellina* sp.) (Takoucht, Aoulkjdad), especially in its upper part (Tinfoul, Tiskatine), suggesting dysaerobic conditions (e.g. Henderson, 2004).

Due to poor outcrop conditions, the identification of the sixth and seventh sequences are still preliminary. The ammonite content of the **sixth sequence** (<20 m) indicates an early Albian age (upper *L. tardefurcata* Zone and *D. mammillatum* Superzone p.p.). In all sections, the lower sequence boundary (D 5, Figs. 5, 8–10) is a S 4B surface. Beside pelagic fauna, the strata overlying D 5 contains a molluscan fauna (brachiopods, pectinids, plicatulids) not as shallow as those overlying D 4, and frequent phosphatized internal molds. Therefore, D 5 may correspond to a submarine erosion period. The fauna is dominated by belemnites, serpulids and plicatulids; some flat ammonites ("Beudanticeras beds") are present in the lower part, and *Aucellina* sp. and serpulids are quite abundant in some sections (Tiskatine, Aoulkjdad, Takoucht, Tamzergout). The latter indicate a clear dysaerobic environment, which may be an equivalent of the organic-rich deposits of the coeval "Niveau Paquier" of southeastern France (Kennedy et al., 2000). The top of the sequence is marked by the increase of sandy beds, suggesting the progradation of a coastal clastic system.

The **seventh sequence** (<30 m) has been identified only in the Tamzergout, Tiskatine, Aoulkjdad and Takoucht sections. Its poor ammonite content indicates an early Albian age (*D. mammillatum* Superzone p.p.). The lower discontinuity (D 6, Figs. 8 and 9) is an erosional surface (S 4B) overlain by a sandstone bed containing phosphate clasts. Sequence 7 consists of sandy/silty marls with abundant sandy limestone and sandstone beds. The fauna is similar to that of the sixth sequence (plicatulids, serpulids, belemnites, *Aucellina* sp., scarce large bivalves). In Tinfoul and Anzate, this sequence is probably present but has not been differentiated from the sixth sequence (Fig. 8). The thickness of the sequence and the amount of detrital quartz and sandstone beds seem to increase toward the North and East (Tinfoul, Aoulkjdad, Takoucht).

An **eighth sequence** is locally partly visible (Addar, Tiskatine, Aoulkjdad, Tamzergout). Its lower boundary (D 7, Figs. 5 and 7) is an S 4B surface. The sandstone bed overlying D 7 contains wood remains, ostreids, frequent lithoclasts, and locally presents parallel laminae and Hummocky Cross Stratification, which suggest a very shallow depositional environment. These features suggest that D 7 may correspond to a subaerial erosion period. This interpretation is substantiated by common plant remains in the abundant sandstone beds of the underlying sequence 7, which suggest the proximity of emergent land. Scarce and little diversified ammonites indicate an early Albian age. The rare faunal content comprises ammonites, belemnites, plicatulids and serpulids in the sandstone beds, and *Aucellina* sp. in the sandy, marly shales. Together with the apparent scarcity of bioturbation, this suggests ongoing dysoxic conditions. The overlying shales are frequently covered. The fifth to eighth sequences constitute the lower part of the Oued Tidzi Fm (Duffaud et al., 1966).

5.2. Comparison with other areas

Although the Aptian period has been extensively studied for paleoenvironmental and paleooceanographic conditions (e.g. Sabatino et al., 2015, and references therein), relatively few works

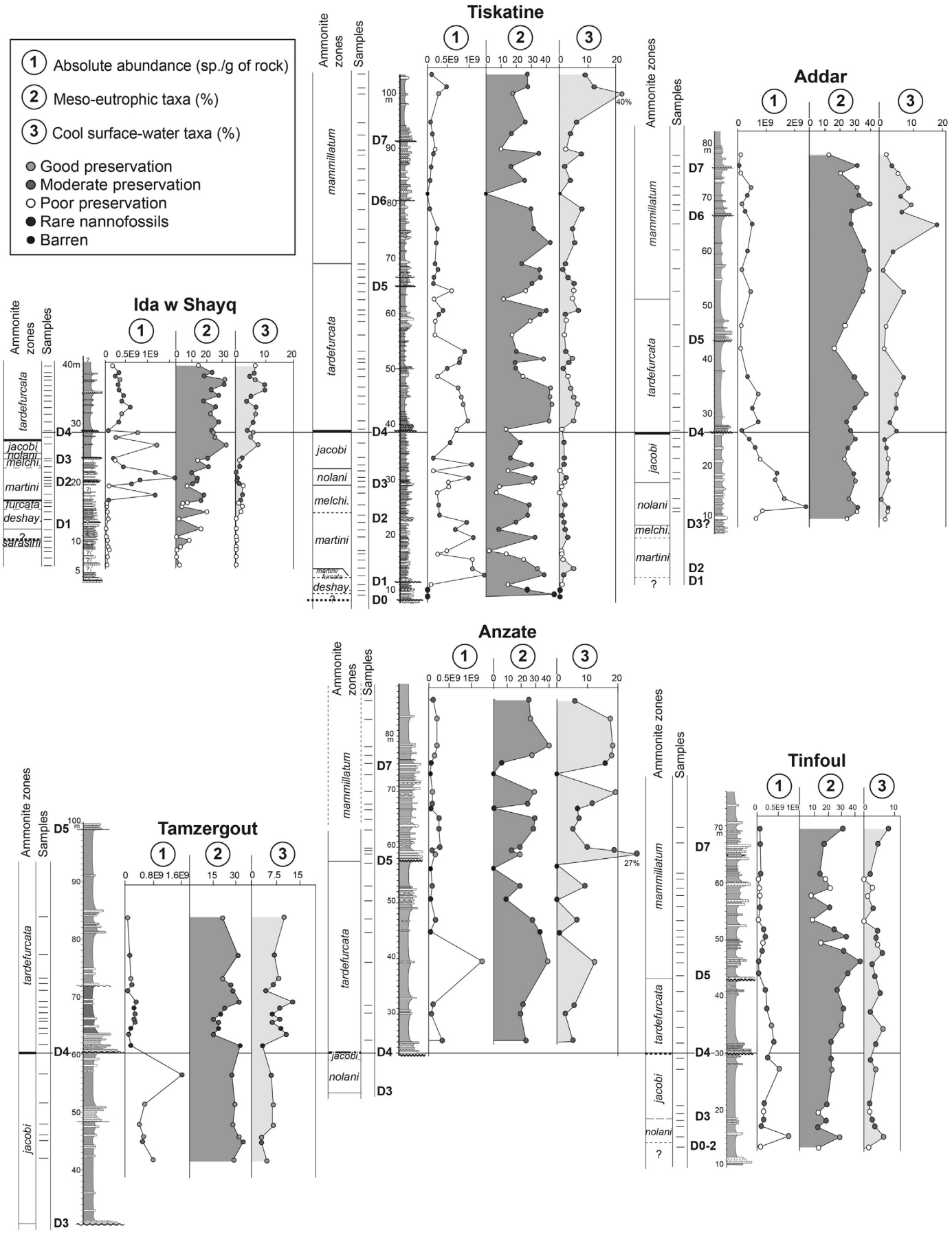

Fig. 7. Stratigraphic changes in calcareous nannofossil total absolute abundance and relative abundances of both meso-eutrophic and cold taxa. The sedimentary discontinuities (D0–D7) are indicated.

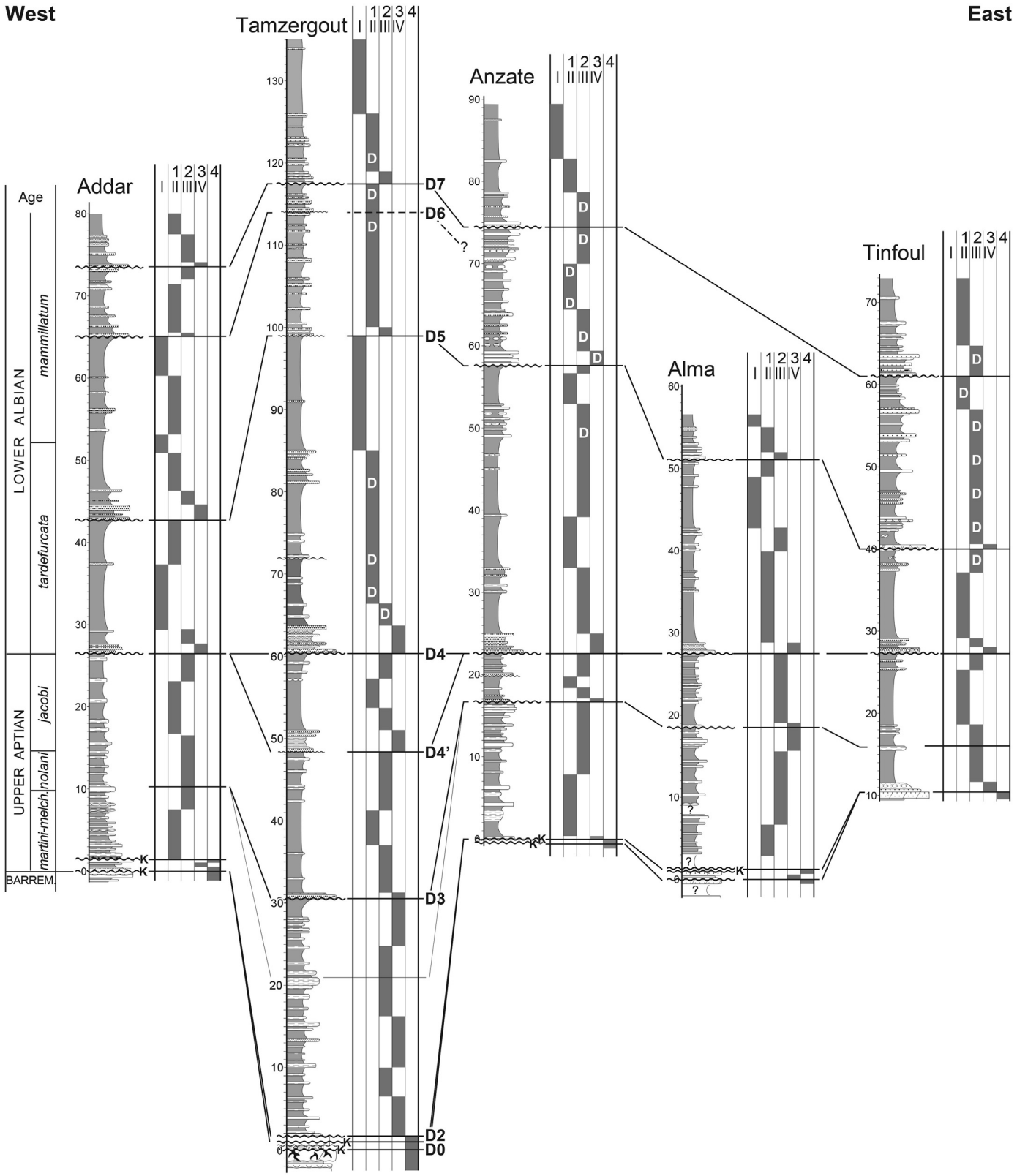

Fig. 8. East-West correlations of the Aptian–lower Albian sections in the southern part of the Essaouira-Agadir basin. D: dysaerobic facies. See Fig. 10 for caption, and Fig. 3 for explanation of 1–4, and I–IV.

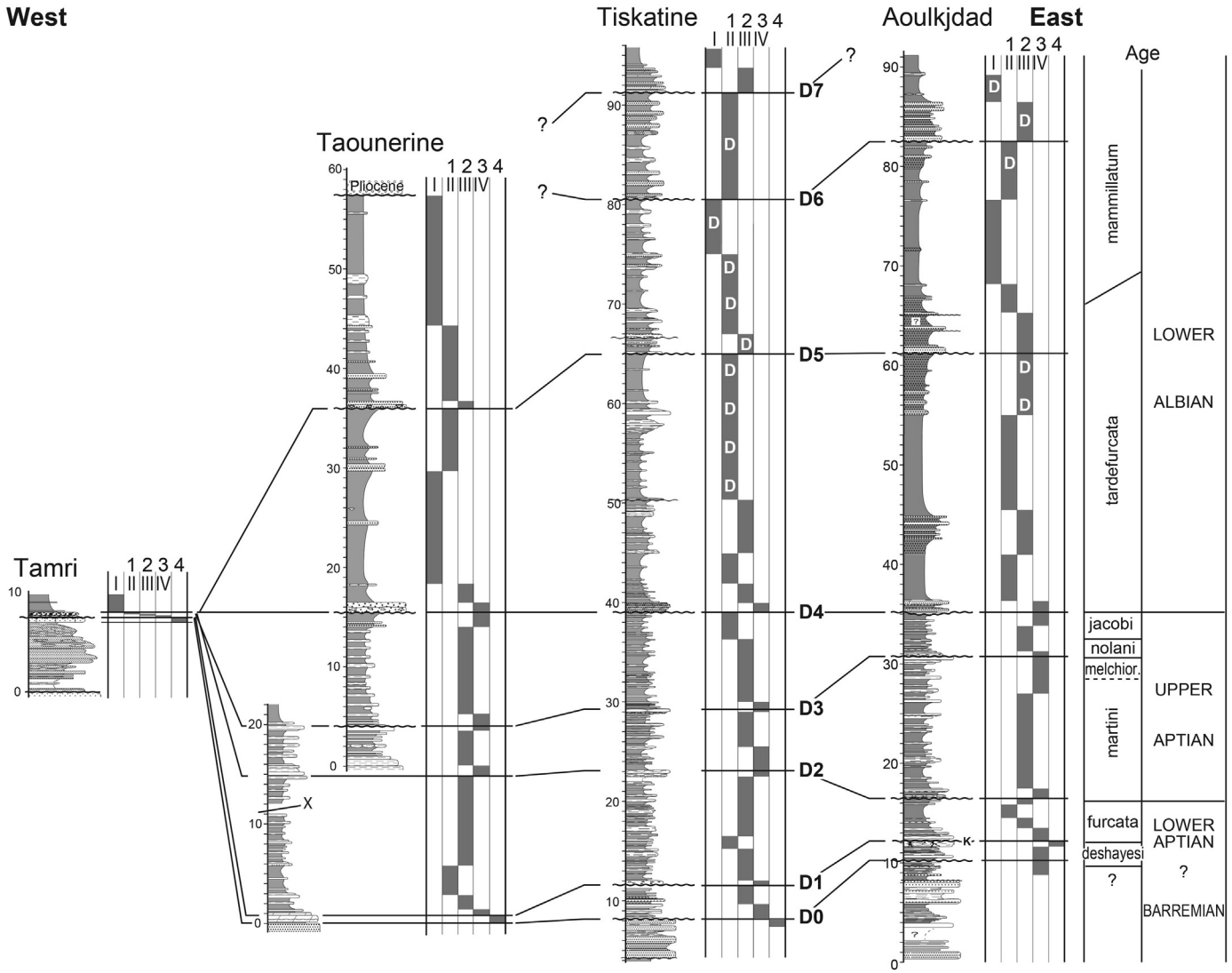

Fig. 9. East-West correlations of the Aptian–lower Albian sections in the central part of the Essaouira-Agadir Basin. D: dysaerobic facies. See Fig. 10 for caption, and Fig. 3 for explanation of 1–4, and I–IV.

are available on the sequence stratigraphy of this stage. A SB of latest Barremian age (within the *Martellites sarrasini* Zone) has been identified in southern (Ruiz-Ortiz and Castro, 1998) and northern Spain (Bover-Arnal et al., 2009), and in the Urgonian platform of the Swiss and French Prealps (Arnaud et al., 1998; Clavel et al., 2013; Tendil et al., 2018), which correlates with our D0. Some authors mentioned a first lower Aptian SB around the limit between the *Deshayesites oglanlensis* and *D. forbesi* ammonite zones (Bover-Arnal et al., 2009; Martín-Martín et al., 2013; Tendil et al., 2018), and a second one between the *D. forbesi* and *D. deshayesi* zones (Ruiz-Ortiz and Castro, 1998; Arnaud et al., 1998; Raddadi, 2004; see also Embry et al., 2010). Because of common condensation and poor sedimentary record, none of these discontinuities has been recognized confidently in the EAB, most probably due to the low sea level globally recorded in earliest Aptian times (e.g. Haq, 2014). A third lower Aptian SB has been dated as close to the *D. deshayesi-Dufrenoyia furcata* ammonite zones boundary (Martín-Martín et al., 2013; H. Arnaud, pers. comm., 2014), which may be correlated with D1. D2, dated as close to the early–late Aptian boundary (*D. furcata-Epicheloniceras martini* zones) is probably coeval with the SB identified in Spain (Bover-Arnal et al., 2009; Embry et al., 2010; Martín-Martín et al., 2013) and in south-eastern France (H. Arnaud, pers. comm., 2014; Pictet et al., 2015). The SB identified in Spain within the *E. martini* and *Parahoplites melchioris* zones (Ruiz-Ortiz and Castro, 1998; Bover-Arnal et al., 2009; Martín-Martín et al., 2013) has been recognized neither in the EAB, nor in southern France (Raddadi, 2004; Clavel et al., 2013). The D3 identified in the EAB is located within the *Acanthohoplites nolani* Zone, and therefore, is correlatable with the SB identified in southern Spain (Ruiz-Ortiz and Castro, 1998), while D4′ seems to be correlatable with the SB identified in the late *Hypacanthoplites jacobi* Zone in Spain (Ruiz-Ortiz and Castro, 1998; Bover-Arnal et al., 2009; Martín-Martín et al., 2013) and Tunisia (Chihaoui et al., 2010; Latil, 2011; Hfaied et al., 2013). D4 of the EAB, the erosional surface of which contains the Aptian–Albian boundary, is easily correlated with the base of the Hameima Fm in Central Tunisia (Chiahoui et al., 2010; Latil, 2011) and with the base of the Alb 1 sequence of Hfaied et al. (2013) in southern Tunisia, both marked by a sedimentary hiatus. In Spain, it probably correlates with the Aptian–Albian boundary of Martin-Martin et al. (2013) and with Sb7 of Ruiz and Castro (1998). As a consequence, and taking into account that poor sedimentary record may have locally limited SB identification in the EAB, the good chronological correlations with other regions of the Tethys suggest that sea-level variations were the main factor controlling

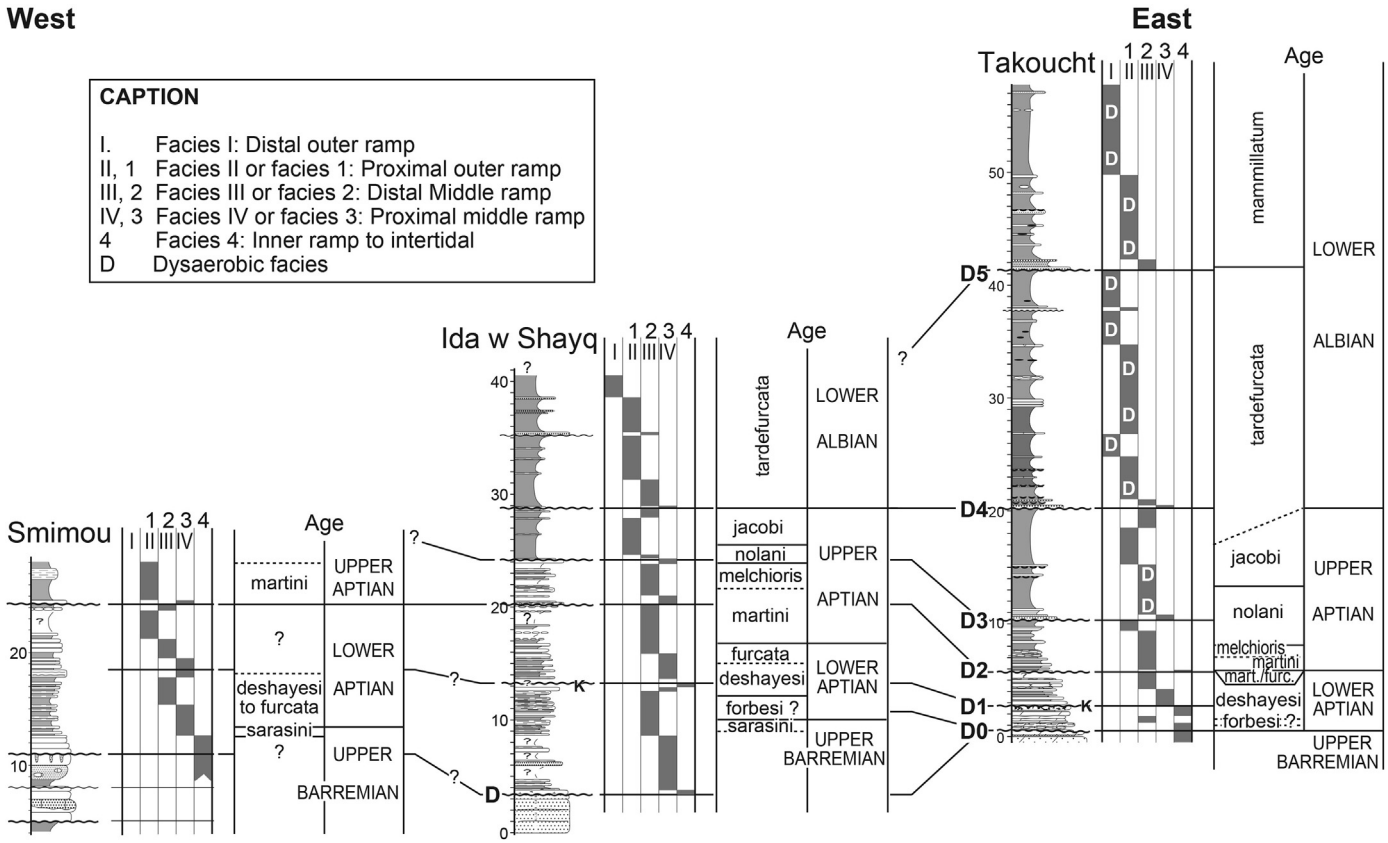

Fig. 10. East-West correlations of the Aptian–lower Albian sections in the northern part of the Essaouira-Agadir Basin. D: dysaerobic facies. See Fig. 3 for explanation of 1–4, and I–IV.

the sedimentary discontinuities in the EAB during Aptian–early Albian times.

5.3. Calcareous nannofossil primary productivity and carbonate production

The nannofossil total absolute abundance depends on primary productivity in the water column, preservation, and sedimentation rate. Significantly lower nannofossil total absolute abundances are observed in Albian than in Aptian strata in samples with different preservation states (poor to good; Fig. 7) and thus do not result from a poor preservation. The decrease in nannofossil total abundance is associated with an increase in the relative abundance of high-fertility nannofossils indicators, which seems contradictory. Indeed, both high nannofossil total abundances and relative abundances of high-fertility taxa can be related to a high primary productivity in marine surface waters. The Aptian lower parts of the sections are more condensed with respect to the lower Albian upper parts, and the change to higher sedimentation rates occurs above D4. Thus, the decrease in nannofossil total absolute abundances recorded in all sections through early Albian times may be explained by an increase in the sedimentation rate, with a dilution effect by the siliciclastic fraction. During the early Albian, enhanced relative abundances of high-fertility taxa suggest an increase in the nannofossil primary productivity.

In a carbonate ramp setting such as the EAB, carbonate production may result from benthic fauna and/or from pelagic organisms, such as calcareous nannofossils. We have investigated more in detail the relationship between nannofossil total abundance and calcium carbonate content. When all data from the different sections are plotted, a correlation exists between these two variables, but remains unclear, especially for high values of calcium carbonate content (>70%) corresponding to Aptian samples (Fig. 11). If the latter values are not taken into account, a low positive correlation ($r = 0.343$, with 162 values and $p < 0.0001$) is observed. This suggests that on the EAB ramp, the carbonate fraction was partly produced by calcareous nannofossils, especially in sediments with values of calcium carbonate content lower than 70%.

The carbonate production was lower for the lower Albian deposits in comparison to the Aptian deposits in the EAB. This is shown by a decrease in the carbonate content starting around D4 (Fig. 6), by a decrease in both semi-quantitative abundance and diversity of shallow marine benthic fauna, and by a decrease in the relative abundances of the bigger calcareous nannofossil calcifier such as *Nannoconus* spp (Fig. 6). The latter is considered as a deep dweller, which is more abundant in marine paleoenvironments with prevailing oligotrophic sea-surface conditions (Table 2). In carbonate oligotrophic environments, the photic zone is supposed to be thicker than in siliciclastic environments, leading deep dweller to develop. This explains that nannoconids 1) are less present in the proximal, more siliciclastic section of Tinfoul with respect to the other sections, and 2) are much more abundant in the upper Aptian carbonate-rich deposits corresponding to low fertility surface waters, with respect to the more siliciclastic deposits that prevailed during the early Albian. Nannoconids are also associated with warm marine paleoenvironments (Table 2). Decrease in their relative abundance in the uppermost Aptian–lower Albian interval may indicate cooler sea-surface temperatures. As a matter of fact, the significant increase in the relative abundance of cold water

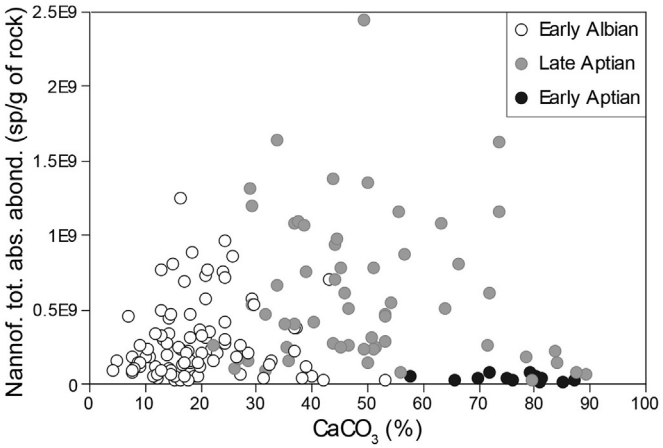

Fig. 11. Bivariate plot showing the relationship between $CaCO_3$ content and calcareous nannofossil absolute abundance for different time intervals, recognized in the Essaouira-Agadir basin. 176 measurements from the Addar, Alma, Anzate, Ida w Shayq, Tinfoul and Tiskatine sections.

nannofossil taxa in the uppermost Aptian, and overall in the lowermost Albian, suggests that cooling occurred, but may be also due to connections with higher latitudes, linked to the recorded sea-level rise. However, connections with higher latitudes cannot explain the decrease in the relative abundance of warm water nannofossil taxa, such as nannoconids. In most of the studied sections the maximum relative abundance of cold water taxa is reached in the early *D. mammillatum* ammonite Superzone. Such sea-water temperature cooling in the late Aptian and earliest Albian is consistent with previous studies in other Tethyan areas (e.g. Bottini et al., 2015; Bodin et al., 2015), although other authors advocated for an ongoing warm climate in parts of the Tethyan realm (see discussion *in* Föllmi, 2012).

5.4. Dynamics of the EAB in Aptian–early Albian times

5.4.1. General statement

Deposition during the Aptian–early Albian was marked in the EAB by an overall low energy environment, as documented by the lack of oolites, coral reefs or grainstone textures. Additionally, the abundance of pyrite in marls, together with the abundant buchidae, suggests that bottom waters were little oxygenated in the middle to distal areas. Facies successions are monotonous and lateral changes are quite gradual. These observations call for a very low-sloped, even ramp topography. The lack of high-energy deposits is probably favoured by the geographic location of the EAB on the western side of a continent. As a matter of fact, in the northern hemisphere, storms are formed in intertropical latitudes and shift first toward the West, due to the trade winds, and then to the North, because of the Coriolis deviation, thus affecting the eastern or southern coasts of the continents. Since the EAB is located on the northwestern margin of Africa, storms were probably scarce, thus favoring a low energy regime and possibly water stratification. Coastal upwelling enhanced by the westward trade winds might have favoured biological activity, resulting in little oxygenation of bottom water in the outer ramp and organic-rich deposition shoreward.

On the other hand, during the late Aptian–early Albian interval, the faunal assemblages were dominated by brachiopods, oysters, plicatulids, pectinids and other bivalves, as well as serpulids, gastropods and irregular urchins. Conversely, they are almost devoid of oolites, oncolites, stromatolites, corals, rudistids and algae. This suggests that, in spite of its intertropical latitude (15–20° lat. N; e.g., Trabucho-Alexandre et al., 2011), the EAB behaved as a temperate platform, at least during late Aptian and early Albian times.

The occurrence of phosphate- and glauconite-rich crusts or clasts suggests that the EAB was submitted to cold, upwelling currents, as documented by Leckie (1984), Herrle et al. (2004), Haydon et al. (2008) and Hofmann et al. (2008) along the Moroccan margin. This interpretation is supported, on one hand by the abundance of glauconite and phosphate clasts in upper Aptian to lower Albian deposits. On the other hand, the westernmost areas (Tamri, Assaka, Imsouane; Figs. 1 and 9) exhibit very condensed sections, where 50 cm-thick, glauconite- and phosphate-rich conglomerates contain ammonites of early Aptian to earliest Albian age. Such a condensation may be attributed to significant, continuous upwelling currents affecting the western edge of the ramp during Aptian to earliest Albian times.

5.4.2. Comparison between Aptian and latest Aptian–early Albian environments

Albian facies differ from the Aptian ones by the abundance of clastic input. A high carbonate production is favoured by a large photic zone, few terrigenous influx, warm sea-surface conditions and slow rise of sea level. Albian facies differ from the Aptian ones by the abundance of detrital input. Aptian deposits comprise marls and limestones, with few, fine grained detrital quartz. Conversely, Albian sedimentation is marked by silty marls and shales, and sandstones. This provoked a change in the overall faunal content. As a matter of fact, pectinids and irregular sea urchins, common in the Aptian beds, are much scarcer in lower Albian deposits, whereas oysters and plicatulids are much more abundant in the latter. In the same way, scarce corals are present in the Aptian succession but are totally absent in the lower Albian series. Although the development of oysters from Albian times onward is a widespread feature that may be related to a global sea-level rise (Dhondt et al., 1999), this suggests also that the lower Albian environment is marked by more important terrigenous sediment supply (local occurrence of plant fragments), and associated nutrients input to the basin, which led to both a reduction of the photic zone depth, and a change from oligotrophic to mesotrophic conditions, illustrated both by increasing calcareous primary productivity and the faunal change. Increasing terrigenous supply was probably caused by enhanced runoff from the emergent continents during more humid climatic conditions. However, the highest nannofossil primary productivity conditions are recorded above D4 (*L. tardefurcata* and lower *D. mammillatum* ammonite Zones), which corresponds to a period of sea-level rise. Therefore, increasing nutrient content could also be due to upwelling conditions developing over the platform during sea-level rise and high sea-level periods.

The average deposition depth seems to have been higher in the early Albian than during the Aptian. During the latter period, the deposition depth varied between 0 m (S 1) and little below the lower limit of the euphotic zone (F 1), whereas in the early Albian, deposition depth varied from the fair weather wave base (F IV), to largely below the euphotic zone (lack of benthic macrofauna in F I). However, this qualitative assessment may be exaggerated, as the more important detrital sediment supply during the early Albian might have reduced the thickness of the photic zone because of repeated clay input into the basin. Therefore, we cannot rule out that facies F II and F III may have been deposited in environments equivalent to, or slightly shallower than, facies F 1 and F 2, respectively.

The average energy level that prevailed during deposition of the lower Albian succession was higher than during the Aptian, as shown by the occurrence in the lower Albian succession of erosional surfaces, dolomitic sandstone beds and current structures in the latter. Since many of these beds overlie erosional surfaces and

thus correspond to drops in sea level, this suggests that these high energy deposits were sedimented in an environment shallower than the storm wave base, or even shallower than the fair weather wave base. This supports the fact that the average deposition depth remained moderate, even during the early Albian.

Finally, the F D facies are restricted to the lower Albian succession, which suggests that the EAB ramp was more oxygen-depleted at that time, than during the Aptian. Two causes may be invoked. On one hand, the O_2 depleted zone may have been too deep to reach the Moroccan ramp during the Aptian, whereas, the higher deposition depth during the early Albian allowed the O_2 depleted zone to reach and impinge upon the EAB. On the other hand, the influence of upwelling currents may have favoured the marine life in the outer zones of the ramp, consuming a part of the available oxygen through biological activity and organic matter degradation, thus favoring the extension of the O_2 depleted zone onto the EAB ramp (e.g. Erbacher et al., 1996; Haydon et al., 2008). One of these O_2 depleted deposits may have been coeval with the OAE1b, since it occurred in Tamzergout during the *L. tardefurcata* ammonite Zone (Peybernès et al., 2013), and has been recognized in Takoucht at the same level (Figs. 5 and 10). There, TOC measurements indicate fluctuations around 1% TOC, but due to the lack of other TOC analysis in other intervals, no comparison can be made.

5.5. Paleogeographic and tectonic evolution

During latest Barremian to earliest late Aptian times (Sequences 1 and 2, *M. sarasini* to *E. martini* p.p. ammonite Zones), the western, southern and eastern areas of the basin are marked by repeated emersions (numerous karstic and epikarstic cavities), which likely produced erosions of part of the previous deposits. As a consequence, Sequences 1 and 2 in these areas are absent or extremely

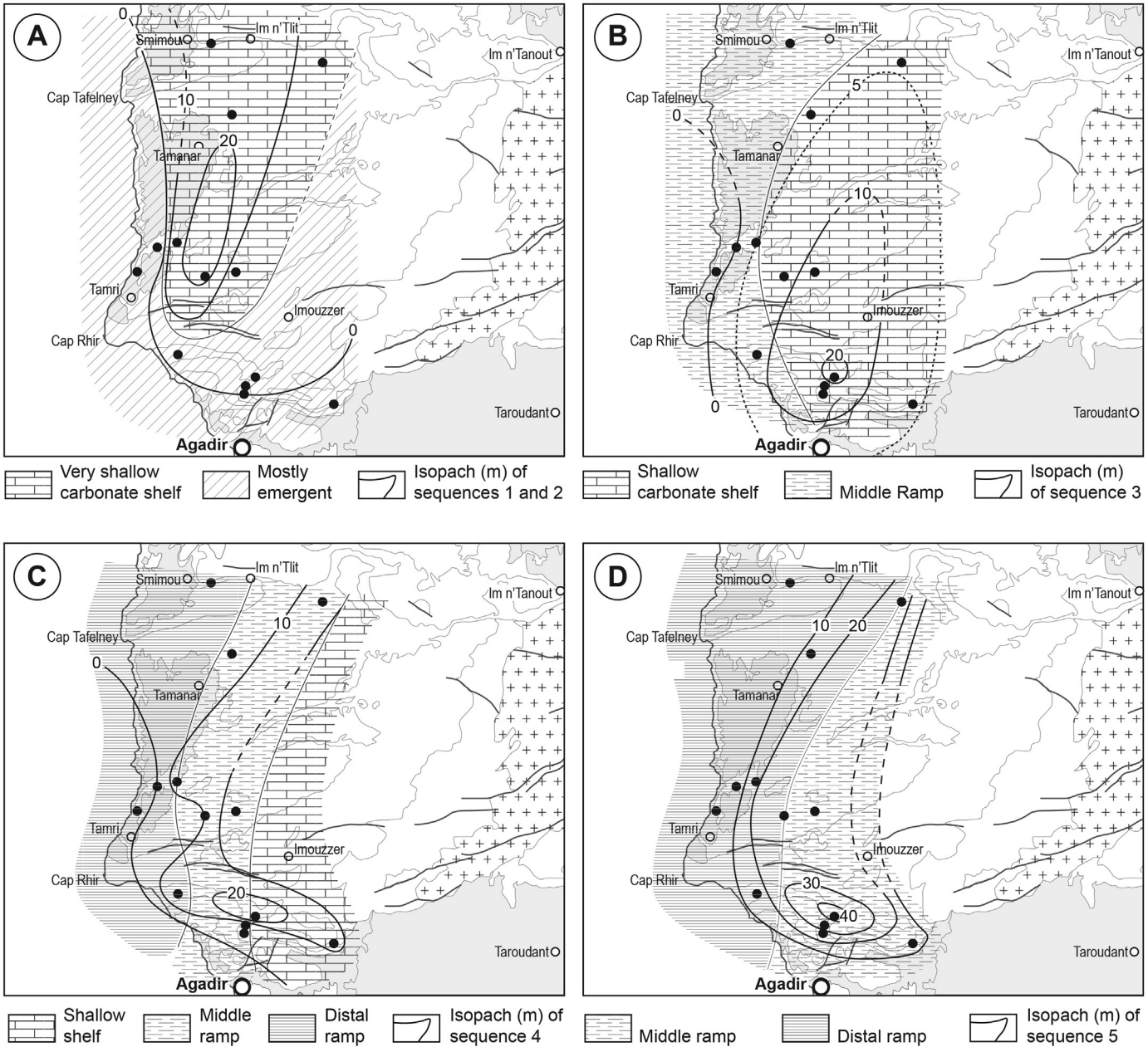

Fig. 12. Paleogeographic and isopach maps of the study area. A. Sequences 1 and 2 (latest Barremian–early Aptian); B. Sequence 3 (early late Aptian); C. Sequence 4 (latest Aptian); D. Sequence 5 (earliest Albian).

reduced. In many sections, however, the occurrence of ammonites shows that marine sedimentation sporadically occurred. Significant carbonate sedimentation only took place in the central part of the EAB (Fig. 12A). This pattern seems inherited from the latest Barremian paleogeography, during which only in the central part of the EAB accumulated a significant thickness of fine-grained marine sandstone ($\approx$5 m), while the western and southern part of the area where submitted to subaerial to submarine condensation (Jaillard et al., 2019). It suggests that the western and southern parts of the EAB were slightly uplifted with respect to the central part around the Barremian–Aptian boundary.

During late Aptian and early Albian times (Sequences 3 to 5), an increase of the depositional depth is recorded by the eastward retrogradation of the sedimentary facies. Shallow marine carbonates were dominant during Sequence 3 and almost disappeared during Sequence 5, whereas outer ramp deposits were absent during Sequence 3 and became predominant during Sequence 5 (Fig. 12B,D). Meanwhile, the southern coastal part of the area (Asaka, Tamri) recorded a submarine condensation (glauconites, phosphate) likely related to upwelling currents, assumed to be active offshore the Moroccan margin in Aptian–Albian times (Herrle et al., 2004; Haydon et al., 2008). Deposition resumed during earliest Albian times, since Sequence 5 is recorded in all studied sections. Note that the Tamzergout area shows a quite localized thickness anomaly, which suggests an anomalous subsidence regime.

During the early Albian, the studied outcrops are unsufficient to allow detailed facies mapping. However, Sequences 6 and 7 (upper *L. tardefurcata* and lower *D. mamillatum* zones) are dominated by outer ramp facies in all areas, including in the southwestern part of the area where the long-lasting submarine condensation ended, and by more homogeneous thicknesses. The thickness anomaly of the Tamzergout area seems to have disappeared.

As a whole, the paleotopography inherited from the late Barremian tectonic event (i.e. uplift of the southern and western areas; Jaillard et al., 2019) seems to be progressively leveled by the lower Aptian accumulation. However, subsidence anomalies are recorded around the present-day Amsittene and Imouzzer anticlines, which are presently underlain by evaporitic diapirs (Mrhidek et al., 2000; Tari and Jabour, 2013). To the north, the Amsittene anticline and its surroundings are marked by a low subsidence regime (Aptian sequences are less than 10 m thick), and to the south, the Imouzzer anticline is first uplifted (Sequences 1 and 2), and then presents an anomalously high subsidence in the Tamzergout section. This localized subsidence anomaly is most likely related to the presence of underlying evaporites, and may be due either to the formation of a rim-syncline or mini-basin located in the vicinity of a rising diapir (e.g. Gilles and Rowan, 2012; Brandes et al., 2012), or to a collapse structure above a karstic system caved in evaporites (e.g. Belderson et al., 1978; Guttiérrez et al., 2008). In the latter interpretation, the occurrence of repeated emersions may have favoured dissolution of evaporite, but the radial or concentric normal faults, commonly associated with these structures (Stewart, 2006), were not observed in the field, neither at small-scale, nor at large-scale. In the former interpretation, the absence of normal faults is frequent in rim-syncline structures, which show locally a ring-shaped morphology or are surrounded by uplifted areas above the rising diapir. These features seem consistent with our data, but more geological observations and surveying are needed to choose between these two interpretations.

6. Conclusions

Our detailed study of the Aptian–lower Albian succession of the EAB allowed to define a biostratigraphic framework, correlated with the standard ammonite zonation of Europe. In this scheme, lowermost Aptian deposits are lacking, lower Aptian strata are poorly represented, and the Aptian–Albian boundary is included within a hiatus marked by a major sedimentary discontinuity.

Careful analysis of sedimentary facies and surfaces made possible to decipher the sedimentary evolution of the EAB during Aptian–early Albian times, and to subdivide this interval into eight depositional sequences. The latter can be correlated with coeval sequences identified in other Tethyan areas, thus suggesting that they were mainly controlled by eustatic variations. In this context, the lack of the lowermost Aptian sequences is most probably related to the significant sea-level fall recorded at that time (Haq, 2014).

As a whole, Aptian–lower Albian deposits of the EAB were accumulated on a low energy ramp that evolved from a carbonate to a mixed carbonate-clastic system. This evolution occurred progressively in Late Aptian times and was associated with an increase of sandy and shaly deposits, with a change from oligotrophic to mesotrophic faunal and nannofossil assemblages, and with and increase of cold water nannofossil taxa indicating a cooling of sea-surface temperatures. Deposition depth seems to be slightly higher in the early Albian than during the Aptian, consistent with the eustatic sea-level rise recorded at that time. The more energetic environment displayed by lower Albian deposits, together with the occurrence of dysaerobic deposits and the abundance of phosphate and glauconite, suggest that upwelling currents were significant in Aptian to early Albian times.

The overall sea-level rise in the late Aptian and early Albian is illustrated by the evolving facies distribution on paleogeographic reconstructions. Furthermore, the latter evidence subsidence anomalies around the present-day anticlines cored by evaporites, thus suggesting the play of mild halokinetic movements during Aptian–early Albian times.

Acknowledgements

Most of the data presented here result from a collaborative programm carried out between the universities of Grenoble, Agadir, Lyon and Marrakech, funded by the Ministries of foreign affairs from France and Morocco (PHC project n° 031/STU/13), which resulted in the achievement of a university thesis (Hassanein, 2016). We benefited from a financial support by the french Institut de Recherche pour le Développement (IRD) to W.H.K. (PhD grant) and E.J. (field trips), and from an annual financial support by the ISTerre, Grenoble, and Terre Planètes Environnement, Lyon, laboratories, and by the OSUG@2020 Labex program of the Observatoire des Sciences de l'Univers de Grenoble. We warmly thank M. Aoutem (Agadir) for his help in field work, F. Baudin (Sorbonne Université) for TOC analysis and interpretation, and J.-L. Latil for fruitful paleontological and biostratigraphic discussions. M. Bernet (Grenoble) is thanked for revising the English text. Sincere thanks are due to Serge Ferry and an anonymous reviewer for their fair and constructive reviews.

References

Al Yacoubi, L., Bouchaou, L., Jaillard, E., Masrour, M., Ait Brahim, Y., El Mouden, A., Schneider, J., Reichert, B., 2017. Impact of rock-water interactions and recharge on water resources quality of the Agadir-Essaouira Basin, Southwestern Morocco. Arabian Journal of Geociences 10, 169. https://doi.org/10.1007/s12517-017-2968-2.

Algouti, A., Algouti, A., Taj-Eddine, K., 1999. Le Sénonien du Haut Atlas occidental, Maroc: sédimentologie, analyse séquentielle et paléogéographie. Journal of African Earth Sciences 29, 643–658.

Ambroggi, R., 1963. Etude géologique du versant méridional du Haut Atlas occidental et de la plaine du Souss. Notes du Service Geologique du Maroc 157, 322.

Ambroggi, R., Breistroffer, M., 1959. Stratigraphie du Crétacé du Haut Atlas Occidental (Sud marocain). In: Congreso Geológico Internacional, Mexico 1956, Sesión XX, n° 157, pp. 33–40.

Andreu, B., 1989. Le Crétacé moyen de la transversale Agadir-Nador (Maroc): précisions stratigraphiques et sédimentologiques. Cretaceous Research 10, 49–80.

Arnaud, H., Arnaud-Vanneau, A., Blanc-Alétru, M.-C., Adatte, T., Argot, M., Delanoy, G., Thieuloy, J.-P., Vermeulen, J., Virgone, A., Virlouvet, B., Wermeille, S., 1998. Répartition stratigraphique des orbitolinidés de la plate-forme urgonienne subalpine et jurassienne (SE de la France). Géologie Alpine 74, 3–89.

Aubry, M.P., Bord, D., Beaufort, L., Kahn, A., Boyd, S., 2005. Trends in size changes in the coccolithophorids, calcareous nannoplankton, during the Mesozoic: a pilot study. Micropaleontology 51, 309–318.

Beaufort, L., 1991. Adaptation of the random settling method for quantitative studies of calcareous nannofossils. Micropaleontology 37, 415–418.

Behar, F., Beaumont, V., De Penteado, H.L.B., 2001. Rock-Eval 6 technology: performances and developments. Oil and Gas Science and Technology 56, 111–134.

Belderson, R.H., Kenyon, N.H., Stride, A.H., 1978. Local submarine salt-karst formation on the Hellenic outer Ridge, eastern Mediterranean. Geology 6, 716–720.

Bertotti, G., Gouiza, M., 2012. Post-rift vertical movements and horizontal deformations in the eastern margin of the Central Atlantic: Middle Jurassic to Early Cretaceous evolution of Morocco. International Journal of Earth Sciences 101, 2151–2165.

Bodin, S., Meissner, P., Janssen, N.M.M., Steuber, T., Mutterlose, J., 2015. Large igneous provinces and organic carbon burial: controls on global temperature and continental weathering during the Early Cretaceous. Global and Planetary Change 131, 238–253.

Bornemann, A., Mutterlose, J., 2006. Size analyses of the coccolith species *Biscutum constans* and *Watznaueria barnesiae* from the Late Albian Niveau Breistroffer (SE France): taxonomic and palaeoecological implications. Geobios 39, 599–615.

Bottini, C., Erba, E., Tiraboschi, D., Jenkyns, H.C., Schouten, S., Sinninghe Damsté, J.S., 2015. Climate variability and ocean fertility during the Aptian stage. Climate of the Past 11, 383–402.

Bourgeoini, Y., Ben Haj Ali, N., Razgallah, S., Tajeddine, K., 2002. Etude biostratigraphique du Crétacé inférieur (Barrémien supérieur-Albien) du Haut Atlas occidental (Maroc). Estudios Geologicos 58, 105–112.

Bover-Arnal, T., Salas, R., Moreno-Bedmar, J.A., Bitzer, K., 2009. Sequence stratigraphy and architecture of a late Early–Middle Aptian carbonate platform succession from the western Maestrat Basin (Iberian Chain, Spain). Sedimentary Geology 219, 280–301.

Bown, P.R., Rutledge, D.C., Crux, J.A., Gallagher, L.T., 1998a. Lower Cretaceous. In: Bown, P.R. (Ed.), Calcareous Nannofossil Biostratigraphy. British Micropalaeontological Society Publications Series. Chapman and Hall/Kluwer Academic Publ., pp. 86–102

Bown, P.R., Young, J.R., 1998b. Techniques. In: Bown, P.R. (Ed.), Calcareous Nannofossil Biostratigraphy. British Micropalaeontological Society Publications Series. Chapman and Hall/Kluwer Academic Publ., pp. 16–28

Brandes, C., Pollok, L., Schmidt, C., Wilde, V., Winseman, J., 2012. Basin modelling of a lignite-bearing rim syncline: insights into rim-syncline evolution and salt diapirsim in NW Germany. Basin Research 24, 699–716.

Brautigam, K., Fernández-Blanco, D., Klaver, J.M., 2009. Late Jurassic-Early Cretaceous Horizontal Tectonics Drives the Jbel Amsittene Anticline in the Haha Basin, Morocco. MSc. Thesis. Free University Amsterdam, p. 59.

Brives, A., 1905. Contribution à l'étude géologique de l'Atlas marocain. Bulletin de la Societe Geologique de France 5, 379–398.

Bulot, L.G., Latil, J.-L., 2014. New insights on the genus *Nolaniceras* Casey, 1961 (Ammonoidea, Cretaceous) and its consequences on the biostratigraphy of the Aptian Stage. Proceedings of the Geologist's Association 125, 227–232.

Burollet, P.F., 1956. Contribution à l'étude stratigraphique de la Tunisie Centrale. Annales des Mines et de la Geologie 18, 350 pp., 22 pl., Tunis.

Busson, G., Noël, D., 1991. Les nannoconidés indicateurs environnementaux des oceans et mers épicontinentales du Jurassique terminal et du Crétacé inférieur. Oceanologica Acta 14, 333–356.

Canérot, J., Cugny, P., Peybernès, B., Rahli, I., Rey, J., Thieuloy, J.-P., 1986. Comparative study of the Lower and Mid-Cretaceous sequences on different maghrebian shelves and basins: Their place in the evolution of the North African, Atlantic and Neotethysian margins. Palaeogeography, Palaeoclimatology, Palaeoecology 55, 213–232.

Chihaoui, A., Jaillard, E., Latil, J.-L., Susperregui, A.-S., Touir, J., Ouali, J., 2010. Stratigraphy of the Hameima and Lower Fahdene formations in the Tajerouine area (Northern Tunisia). Journal of African Earth Sciences 58, 387–399.

Clavel, B., Conrad, M.-A., Busnardo, R., Charollais, J., Granier, B., 2013. Mapping the rise and demise of Urgonian platforms (Late Hauterivian – Early Aptian) in southeastern France and the Swiss Jura. Cretaceous Research 39, 29–46.

Coccioni, R., Erba, E., Premoli Silva, I., 1992. Barremian-Aptian calcareous plankton biostratigraphy from the Gorgo a Cerbara section (Marche, Central Italy) and implication for planktonic evolution. Cretaceous Research 13, 517–537.

Crux, J.A., 1991. Albian calcareous nannofossils from the Gault Clay of Munday's Hill (Bedforshire, England). Journal of Micropalaeontology 10, 203–221.

Davison, I., Davy, P., 2010. Salt tectonics in the Cap Boudjour Area, Aaiun basin, NW Africa. Marine and Petroleum Geology 27, 435–441.

De la Mora, A., Olóriz, F., González-Arreola, C., 2000. «Autochtonous» bivalve assemblages and palaeoecological interpretation in the Upper Jurassic-Lower Cretaceous La Caja Formation from the Cañón de San Matías (Zacatecas, México). Comptes Rendus de l'Académie des Sciences Paris, Earth and Planetary Sciences 331, 741–747.

Dellisanti, F., Pini, G.A., Baudin, F., 2010. Use of Tmax as a thermal maturity indicator in orogenic successions and comparison with clay mineral evolution. Clay Minerals 45, 115–746.

Dhondt, A.V., Malchus, N., Boumaza, L., Jaillard, E., 1999. Cretaceous oysters from North Africa; origin and distribution. Bulletin de la Societe Geologique de France 170, 67–76.

Duffaud, F., Brun, L., Plauchut, B., 1966. Le bassin du Sud-Ouest marocain. In: Reyre, D. (Ed.), Bassins sédimentaires du Littoral africain, 1ère partie. Firmin Didot Publ., Paris, pp. 5–12.

Eleson, J.W., Bralower, T.J., 2005. Evidence of changes in surface water temperature and productivity at the Cenomanian/Turonian Boundary. Micropaleontology 51, 319–332.

Embry, J.-C., Vennin, E., Van Buchem, F.S.P., Schroeder, R., Pierre, C., Aurell, M., 2010. Sequence stratigraphy and carbon isotope stratigraphy of an Aptian mixed carbonate-siliciclastic platform to basin transition (Galve sub-basin, NE Spain). Geological Society, London, Special Publication 329, 113–143.

Erba, E., 1987. Mid-Cretaceous cyclic pelagic facies from the Umbrian-Marchean Basin: what do calcareous nannofossils suggest? International Nannoplankton Association Newsletter 9, 52–53.

Erba, E., 1992. Middle Cretaceous calcareous nannofossils from the western Pacific (Leg 129): evidence for paleoequatorial crossings. In: Larson, R.L., Lancelot, Y., et al. (Eds.), Proceedings of the Ocean Drilling Program, Scientific Results, vol. 129, pp. 189–201.

Erba, E., 1994. Nannofossils and superplumes: the early Aptian "nannoconid crisis". Paleoceanography 9, 483–501.

Erba, E., Guasti, G., Castradori, D., 1989. Calcareous nannofossils record fertility and temperature cycles: evidence from the Albian Gault Clay Formation. INA Newsletter 11, 57–58.

Erba, E., Castradori, D., Guasti, G., Ripepe, M., 1992. Calcareous nannofossils and Milankovitch cycles: the example of the Albian Gault Clay Formation (southern England). Palaeogeography, Palaeoclimatology, Palaeoecology 93, 47–69.

Erbacher, J., Thurow, J., Littke, R., 1996. Evolution patterns of radiolaria and organic matter variations: a new approach to identify sea-level changes in mid-Cretaceous pelagic environments. Geology 24, 499–502.

Espitalié, J., Deroo, G., Marquis, F., 1985/1986. La pyrolyse Rock-Eval et ses applications. Revue de l'Institut Français du Pétrole 40, 563–579, 775–784; 41, 73–89.

Ettachfini, E.M., Souhlel, A., Andreu, B., Caron, M., 2005. La limite Cénomanien-Turonien dans le Haut Atlas central, Maroc. Geobios 38, 57–68.

Föllmi, K., 2012. Early Cretaceous life, climate and anoxia. Cretaceous Research 35, 230–357.

Frizon de Lamotte, D., Saint Bezar, B., Bracène, R., 2000. The two main steps of the Atlas building and geodynamics of the western Mediterranean. Tectonics 19, 740–761.

Frizon de Lamotte, D., Zizi, M., Missenard, Y., Hafid, M., El Azzouzi, M., Maury, R.C., Charrière, A., Taki, Z., Benammi, M., Micard, A., 2008. The Atlas system. In: Michard, A., et al. (Eds.), Continental Evolution: The Geology of Morocco. Lecture Notes in Earth Sciences, vol. 116, pp. 133–202.

Frizon de Lamotte, D., Raulin, C., Mouchot, N., Wrobel-Daveau, J.-C., Blanpied, C., Ringenbach, J.-C., 2011. The southernmost margin of the Tethys realm during the Mesozoic and Cenozoic: initial geometry and timing of the inversion processes. Tectonics 30, TC3002. https://doi.org/10.1029/2010TC002691.

Geisen, M., Bollmann, J., Herrle, J.O., Mutterlose, J., Young, J.R., 1999. Calibration of the random settling technique for calculation of absolute abundances of calcareous nannoplankton. Micropaleontology 45, 437–442.

Gentil, L., 1905. Observations géologiques dans le sud marocain. Bulletin de la Societe Geologique de France 5, 521–523.

Giles, K.A., Rowan, M.G., 2012. Concepts in halokinetic-sequence deformation and stratigraphy. Geological Society, London, Special Publication 363, 7–31.

Giorgioni, M., Keller, C.E., Weissert, H., Hochuli, P.A., Bernasconi, S.M., 2015. Black shales – from coolhouse to greenhouse (early Aptian). Cretaceous Research 56, 716–731.

Giraud, F., Olivero, D., Baudin, F., Reboulet, S., Pittet, B., Proux, O., 2003. Minor changes in surface water fertility across the Oceanic Anoxic Event 1d (latest Albian, SE France) evidenced by calcareous nannofossils. International Journal of Earth Sciences 92, 267–284.

Guiraud, R., Bosworth, W., 1997. Senonian inversion and rejuvenation of rifting in Africa and Arabia: synthesis and implications to plate-scale tectonics. Tectonophysics 282, 39–82.

Gutiérrez, F., Calaforra, J.M., Cardona, F., Ortí, F., Durán, J.J., Garay, P., 2008. Geological and environmental implications of the evaporite karst in Spain. Environmental Geology 53, 951–965.

Hafid, M., Aït Salem, A., Bally, A.W., 2000. The western termination of the Jebilet-High Atlas system (offshore Essaouiara Basin, Morocco). Marine and Petroleum Geology 17, 431–443.

Hafid, M., Tari, G., Bouhadioui, D., El Moussaid, I., Aït Salem, A., Nahim, M., Dakki, M., 2008. Atlantic Basins. In: Michard, A., et al. (Eds.), Continental Evolution: the Geology of Morocco. Lecture Notes in Earth Sciences, vol. 116, pp. 303–329.

Haq, B.U., 2014. Cretaceous eustasy revisited. Global and Planetary Change 113, 44–58.

Hassanein, W., 2016. The Aptian–Albian Transgression in the Agadir-Essaouira Basin, Western Morocco. PhD Thesis. University Grenoble Alpes, p. 308.

Haydon, M., Adatte, T., Keller, G., Bartels, D., Föllmi, K.B., Steinamnn, P., Berner, Z., Chellai, E.H., 2008. Organic deposition and phosphorus accumulation during Oceanic Anoxic Event 2 in Tarfaya, Morocco. Cretaceous Research 29, 1008–1023.
Henderson, R.A., 2004. A mid-Cretaceous association of shell beds and organic-rich shale: bivalve exploitation of a nutrient-rich, anoxic sea-floor environment. Palaios 19, 156–169.
Herrle, J.O., Kössler, P., Friedrich, O., Erlenkeuser, H., Hemleben, C., 2004. High-resolution carbon isotope records of the Aptian to Lower Albian from SE France and the Mazagan Plateau (DSDP Site 545): a stratigraphic tool for paleoceanographic and paleobiologic reconstruction. Earth and Planetary Science Letters 218, 149–161.
Hfaied, R., Arnaud-Vanneau, A., Godet, A., Arnaud, H., Zghal, I., Ouali, J., Latil, J.-L., Jallali, H., 2013. Biostratigraphy, palaeoenvironments and sequence stratigraphy of the Aptian sedimentary succession at Jebel Bir Oum Ali (Northern Chain of Chotts, South Tunisia): Comparison with contemporaneous Tethyan series. Cretaceous Research 46, 177–207.
Hofmann, P., Stüsser, I., Wagner, T., Schouten, S., Sinninghe Damsté, J.S., 2008. Climate-ocean coupling off North-West Africa during the Lower Albian: the Oceanic Anoxic Event 1b. Palaeogeography, Palaeoclimatology, Palaeoecology 262, 157–165.
Jaillard, E., Al Yacoubi, L., Reboulet, S., Robert, E., Masrour, M., Bouchaou, L., Giraud, F., El Hariri, K., 2019. Late Barremian eustacy and tectonism in the western High Atlas (Essaouira-Agadir Basin), Morocco. Cretaceous Research 93, 225–244.
Jati, M., Grosheny, D., Ferry, S., Masrour, M., Aoutem, M., Içame, N., Gauthier-Lafaye, F., Desmares, D., 2010. The Cenomanian-Turonian boundary event on the Moroccan Atlantic margin (Agadir basin): stable isotope and sequence stratigraphy. Palaeogeography, Palaeoclimatology, Palaeoecology 296, 151–164.
Kennedy, W.J., Gale, A.S., Bown, P.R., Caron, M., Davey, R.J., Gröcke, D., Wray, D.S., 2000. Integrated stratigraphy across the Aptian-Albian boundary in the Marnes Bleues, at the Col de Pré-Guittard, Arnayon (Drôme), and at Tartonne (Alpes-de-Haute-Provence), France: a candidate global boundary stratotype section and boundary point for the base of the Albian stage. Cretaceous Research 21, 591–720.
Kennedy, W.J., Gale, A.S., Huber, B.T., Petrizzo, M.R., Bown, P., Barchetta, A., Jenkyns, H.C., 2014. Integrated stratigraphy across the Aptian/Albian boundary at Col de Pré-Guittard (southeast France): a candidate global boundary stratotype section. Cretaceous Research 51, 248–259.
Kilian, W., Gentil, L., 1906. Découverte de deux horizons crétacés remarquables au Maroc. Comptes rendus sommaire de l'Académie des Sciences de Paris 142, 603–605.
Kilian, W., Gentil, L., 1907. Sur les terrains crétacés de l'Atlas Occidental marocain. Comptes rendus sommaire de l'Académie des Sciences de Paris 144, 49–51.
Klingelhoefer, F., Biari, Y., Sahabi, M., Aslamnian, D., Schnabel, M., Matias, L., Benabdellouahed, M., Funck, T., Gutscher, M.-A., Reichert, C., Austin, J.A., 2016. Crustal structure variations along the NW-African continental margin: a comparison of new and existing models from wide-angle and reflection seismic data. Tectonophysics 674, 227–252.
Kuroda, J., Tanimizu, M., Hori, R.S., Suzuki, K., Ogawa, N.O., Tejada, M., Coffin, M.F., Coccioni, R., Erba, E., Ohkouchi, N., 2011. Lead isotopic record of Barremian–Aptian marine sediments: implications for large igneous provinces and the Aptian climatic crisis. Earth and Planetary Science Letters 307, 126–134.
Latil, J.-L., 2011. Lower Albian ammonites from Central Tunisia and adjacent areas of Algeria. Revue de Paléobiologie 30, 321–429.
Leckie, R.M., 1984. Mid-Cretaceous planktonic foraminiferal biostratigraphy off Central Morocco, Deep Sea Drilling Project Leg 79, Sites 545 and 547. In: Hinz, K., Winterer, E.L., et al. (Eds.), Initial Reptorts DSDP, vol. 79. U.S. Govt. Printing Office, Washington, pp. 579–620.
Lees, J.A., 2002. Calcareous nannofossil biogeography illustrates palaeoclimate change in the Late Cretaceous Indian Ocean. Cretaceous Research 23, 537–634.
Lemoine, P., 1905. Mission dans le Maroc occidental, Automne 1904, rapport au Comité du Maroc. Comité du Maroc, Paris, p. 223.
Linnert, C., Mutterlose, J., Erbacher, J., 2010. Calcareous nannofossils of the Cenomanian-Turonian boundary interval from the Boreal Realm (Wunstorf, northwest Germany). Marine Micropaleontology 74, 38–58.
Luber, T.L., Bulot, L.G., Redfern, J., Frau, C., Arantegui, A., Masrour, M., 2017. A revised ammonoid biostratigraphy for the Aptian of NW Africa: Essaouira-Agadir Basin. Cretaceous Research 79, 12–34.
Luber, T.L., Bulot, L.G., Redfern, J., Nahim, M., Jeremiah, J., Simmons, M., Bodin, S., Frau, C., Bidgood, M., Masrour, M., 2019. A revised chronostratigraphic framework for the Aptian of the Essaouira-Agadir Basin, a candidate type section for the NW African Atlantic Margin. Cretaceous Research 93, 292–317.
Martín-Martín, J.D., Gomez-Rivas, E., Bover-Arnal, T., Travé, A., Salas, R., Moreno-Bedmar, J.A., Tomás, S., Corbella, M., Teixell, A., Vergès, J., Stafford, S.L., 2013. The Upper Aptian to Lower Albian syn-rift carbonate succession of the southern Maestrat Basin (Spain): facies architecture and fault controlled stratabound dolostones. Cretaceous Research 41, 217–236.
Masrour, M., Aoutem, M., Atrops, F., 2004. Succession des peuplements d'échinides du Crétacé inférieur dans le Haut Atlas atlantique (Maroc); révision systématique et intérêt stratigraphique. Geobios 37, 595–617.
Moulin, M., Aslanian, D., Unternehr, P., 2010. A new starting point for the South and Equatorial Atlantic Ocean. Earth-Science Reviews 98, 1–37.
Mridekh, A., Toto, E.A., Hafid, M., El Ouataoui, A., 2000. Structure sismique de la plate-forme Atlantique au large d'Agadir (Maroc sud-occidental). Comptes rendus de l'Académie des sciences, Paris, Earth and Planet Sciences, Géodynamique 331, 387–392.
Müller, G., Gastner, M., 1971. The "Karbonat-Bombe", a simple device for the determination of the carbonate content in sediments, soils and other materials. Neues Jahrbuch für Mineralogie – Monathefte 10, 466–469.
Mutterlose, J., 1989. Temperature-controlled migration of calcareous nannofloras in the north-west European Aptian. In: Crux, J.A., van Heck, S.E. (Eds.), Nannofossils and Their Applications. Ellis Horwood, Chichester, pp. 122–142.
Mutterlose, J., 1992a. Lower Cretaceous nannofossil biostratigraphy off northwestern Australia (Leg 123). In: Gradstein, F.M., Ludden, J.N. (Eds.), Proceedings of the Ocean Drilling Program, vol. 123. Scientific Results, pp. 343–368.
Mutterlose, J., 1992b. Biostratigraphy and palaeobiogeography of Early Cretaceous calcareous nannofossils. Cretaceoud Research 13, 167–189.
Mutterlose, J., Kessels, K., 2000. Early Cretaceous calcareous nannofossils from high latitudes: implications for palaeobiogeography and palaeoclimate. Palaeogeography, Palaeoclimatology, Palaeoecology 160, 347–372.
Pauly, S., Mutterlose, J., Alsen, P., 2012. Lower Cretaceous (upper Ryazanian-Hauterivian) chronostratigraphy of high latitudes (North-East Greenland). Cretaceous Research 34, 308–326.
Perch-Nielsen, K., 1985. Mesozoic calcareous nannofossils. In: Bolli, H.M., Saunders, J.B., Perch-Nielsen, K. (Eds.), Plankton Stratigraphy. Cambridge University Press, pp. 329–426.
Peybernès, C., Giraud, F., Jaillard, E., Robert, E., Masrour, M., Aoutem, M., Içame, N., 2013. Calcareous nannofossil productivity and carbonate production on the southern Tethyan margin (Morocco) during the Late Aptian-Early Albian: paleoclimatic implications. Cretaceous Research 39, 149–169.
Pictet, A., Delanoy, G., Adatte, T., Spangenberg, J.E., Beaudouin, C., Boselli, P., Boselli, M., Kindler, P., Föllmi, K.B., 2015. Three successive phases of platform demise during the early Aptian and their association with the oceanic anoxic Selli episode (Ardèche, France). Palaeogeography, Palaeoclimatology, Palaeoecology 418, 101–125.
Premoli Silva, I., Erba, E., Tornaghi, M.E., 1989. Paleoenvironmental signals and changes in surface fertility in Mid Cretaceous Corg-rich pelagic facies of the Fucoid Marls (Central Italy). Geobios 11, 225–236.
Raddadi, M.C., 2004. Etude de la nature de la radioactivité gamma dans les roches carbonatées de plate-forme: analyses et interprétations environnementales, diagénétiques et géodynamiques. Géologie Alpine, Mémoire hors série 45, 168.
Reboulet, S., et al., 2018. Report on the 6th International Meeting of the IUGS Lower Cretaceous Ammonite Working Group, the Kilian Group (Vienna, Austria, 20th August 2017). Cretaceous Research 91, 100–110.
Rey, J., Canérot, J., Peybernès, B., Taj-Eddine, K., Rahhali, I., Thieuloy, J.-P., 1986. Le Crétacé inférieur de la région d'Essaouira: données biostratigraphiques et évolutions sédimentaires. PICG – UNESCO section Sciences de la Terre 183. Revue de la Faculté des sciences de Marrakech, numéro spécial 2, 413–441.
Rey, J., Canérot, J., Peybernès, B., Taj-Eddine, K., Thieuloy, J.-P., 1988. Lithostratigraphy, biostratigraphy and sedimentary dynamics of the Lower Cretaceous deposits on the northern side of the western High Atlas (Morocco). Cretaceous Research 9, 141–158.
Roch, E., 1930. Histoire stratigraphique du Maroc. Notes et Mémoires du Service géologique du Maroc 80, 440.
Roth, P.H., 1981. Mid-Cretaceous calcareous nannoplankton from the Central Pacific: implications for paleoceanography. In: Thiede, J., et al. (Eds.), Initial Reports of the Deep Sea Drilling Project, vol. 62, pp. 471–489.
Roth, P.H., 1983. Jurassic and Lower Cretaceous calcareous nannofossils in the western North Atlantic (Site 534): biostratigraphy, preservation, and some observations on biogeography and paleoceanography. In: Sheridan, R.E., Gradstein, F.M., et al. (Eds.), Initial Reports of the Deep Sea Drilling Project 76. U.S. Government Printing Office, Washington, pp. 587–621.
Roth, P.H., 1989. Ocean circulation and calcareous nannoplankton evolution during the Jurassic and Cretaceous. Palaeogeography, Palaeoclimatology, Palaeoecology 74, 111–126.
Roth, P.H., Bowdler, J., 1981. Middle Cretaceous nannoplankton biogeography and oceanography of the Atlantic Ocean. In: Warme, J.E., Douglas, R.G., Winterer, E.L. (Eds.), The Deep Sea Drilling Project: a Decade of Progress, vol. 32. SEPM. Sp. Publ., pp. 517–546
Roth, P.H., Krumbach, K.P., 1986. Middle Cretaceous calcareous nannofossil biogeography and preservation in the Atlantic and Indian Oceans: Implications for paleoceanography. Marine Micropaleontology 10, 235–266.
Ruiz-Ortiz, P.A., Castro, J.M., 1998. Depositional sequences in shallow to hemipelagic platform deposits; Aptian, Prebetic, Alicante (SE Spain). Bulletin de la Societe Geologique de France 169, 21–33.
Sabatino, N., Coccioni, R., Manta, D.S., Baudin, F., Vallefuoco, M., Traina, A., Sprovieri, M., 2015. High-resolution chemostratigraphy of the late Aptian–early Albian oceanic anoxic event (OAE 1b) from the Poggio le Guaine section (Umbria–Marche Basin, central Italy). Palaeogeography, Palaeoclimatology, Palaeoecology 426, 319–333.
Scarparo Cunha, A.A., Shimabukuro, I., 1997. *Braarudosphaera* blooms and anomalous enrichment of *Nannoconus*: evidence from Turonian South Atlantic, Santos Basin, Brazil. Journal of Nannoplankton Research 19, 51–55.
Schettino, A., Turco, E., 2009. Breakup of Pangaea and plate kinematics of the central Atlantic and Atlas regions. Geophysical Journal International 178, 1078–1097.
Schlager, W., 2003. Benthic carbonate factories of the Phanerozoic. International Journal of Earth Sciences 92, 445–464.

Schlanger, S.O., Jenkyns, H.C., 1976. Oceanic anoxic events: causes and consequences. Geologie en Mijnbouw 55, 179–184.
Skelton, P.W., Gili, E., 2012. Rudists and carbonate platforms in the Aptian: a case study on biotic interactions with ocean chemistry and climate. Sedimentology 59, 81–117.
Stets, J., 1992. Mid-Jurassic events in the Western High Atlas (Morocco). Geologische Rundschau 81, 68–84.
Stewart, S.A., 2006. Implications of passive salt diapir kinematics for reservoir segmentation by radial and concentric faults. Marine and Petroleum Geology 23, 843–853.
Street, C., Bown, P.R., 2000. Palaeobiogeography of early Cretaceous (Berriasian-Barremian) calcareous nannoplankton. Marine Micropaleontology 39, 265–291.
Tappan, H.L., 1980. The Paleobiology of Plant Protists, p. 1028. San Francisco.
Tari, G., Jabour, H., 2013. Salt tectonics along the Atlantic margin of Morocco. Geological Society, London, Special Publications 369, 337–353.
Tendil, A.J.-B., Frau, C., Léonide, P., Fournier, F., Borgomano, J.R., Lanteaume, C., Masse, J.-P., Masonnat, G., Rolando, J.-P., 2018. Platform-to-basin anatomy of a Barremian-Aptian Tethyan carbonate system: new insights into regional factors controlling the stratigraphic architecture of the Urgonian Provence platform (southeast France). Cretaceous Research 91, 382–411.
Trabucho-Alexandre, J., von Gilst, R.I., Rodríguez-López, J.P., de Boer, P.L., 2011. The sedimentary expression of oceanic anoxic event 1b in the North Atlantic. Sedimentology 58, 1217–1246.
Tucker, M.E., Wright, V.P., 1990. Carbonate Sedimentology. Blackwell, Oxford, p. 496.
Vila, J.-M., 1980. La chaîne alpine d'Algérie orientale et des confins algéro-tunisiens. Thèse Doctorat ès Sciences. Univ. Pierre et Marie Curie, Paris VI, 665 pp., 40 pl., 3 vol.
Watkins, D.K., 1989. Nannoplankton productivity fluctuations and rhythmically-bedded pelagic carbonates of the Greenhorn Limestone (Upper Cretaceous). Palaeogeography, Palaeoclimatology, Palaeoecology 74, 75–86.
Watkins, D.K., Wise, S.W., Pospichal, J.J., Crux, J., 1996. Upper Cretaceous calcareous nannofossil biostratigraphy and paleoceanography of the Southern Ocean. In: Moguilevski, A., Whatley, R. (Eds.), Microfossils and Oceanic Environments, University of Wales. Aberystwyth Press, pp. 355–381.
Wiedmann, J., Butt, A., Einsele, G., 1978. Vergleich von marokkanischen Kreide-Küstenaufschlüssen und Tiefseebohrungen (DSDP): stratigraphie, Paläonenvironment und Subsidenz an einem passive Kontinentalrand. Geologische Rundschau 67, 454–508.
Wiedmann, J., Butt, A., Einsele, G., 1982. Cretaceous stratigraphy, environment, and subsidence history at the Moroccan continental margin. In: von Rad, U., et al. (Eds.), Geology of the Northwest African Continental Margin. Springer-Verlag, pp. 366–395.
Williams, J.R., Bralower, T.J., 1995. Nannofossil assemblages, fine fraction isotopes, and the paleoceanography of the Valanginian-Barremian (Early Cretaceous) North Sea Basin. Paleoceanography 10, 815–839.
Wise, S.W., 1988. Mesozoic-Cenozoic history of calcareous nannofossils in the region of the Southern Ocean. Palaeogeography, Palaeoclimatology, Palaeoecology 67, 157–179.
Witam, O., 1998. Le Barrémien-Aptien de l'Atlas Occidental (Maroc): lithostratigraphie, biostratigraphie, sédimentologie, stratigraphie séquentielle, géodynamique et paléontologie. Strata 30, 1–421.
Zühlke, R., Bouaouda, M.-S., Ouajhain, B., Bechstädt, T., Leinfelder, R., 2004. Quantitative Meso/Cenozoic development of the eastern Central Atlantic continental Shelf, western High Atlas, Morocco. Marine and Petroleum Geology 21, 225–276.

Appendix A. Supplementary data

Supplementary data to this article can be found online at https://doi.org/10.1016/j.cretres.2019.04.008.